White Rose Research Online

eprints@whiterose.ac.uk
https://eprints.whiterose.ac.uk
Universities of Leeds, Sheffield and York

Deposited via The University of Leeds.

White Rose Research Online URL for this paper:
https://eprints.whiterose.ac.uk/id/eprint/90144/

Version: Accepted Version

**Article:**
Economou, A, Gomez Corral, A and Lopez Garcia, M (2015) A stochastic SIS epidemic model with heterogeneous contacts. Physica A: Statistical Mechanics and its Applications, 421. pp. 78-97. ISSN: 0378-4371

https://doi.org/10.1016/j.physa.2014.10.054

© 2014, Elsevier. Licensed under the Creative Commons Attribution-NonCommercial-NoDerivatives 4.0 International http://creativecommons.org/licenses/by-nc-nd/4.0/

**Reuse**
Items deposited in White Rose Research Online are protected by copyright, with all rights reserved unless indicated otherwise. They may be downloaded and/or printed for private study, or other acts as permitted by national copyright laws. The publisher or other rights holders may allow further reproduction and re-use of the full text version. This is indicated by the licence information on the White Rose Research Online record for the item.

**Takedown**
If you consider content in White Rose Research Online to be in breach of UK law, please notify us by emailing eprints@whiterose.ac.uk including the URL of the record and the reason for the withdrawal request.

UNIVERSITY OF LEEDS
University of Sheffield
UNIVERSITY of York

# A stochastic SIS epidemic model with heterogeneous contacts

A. Economou[a,*], A. Gómez-Corral[b,c], M. López García[d]

[a] *Section of Statistics and Operations Research, Department of Mathematics, University of Athens, Panepistemiopolis, Athens 15784, Greece*
[b] *ICMAT – Institute of Mathematical Sciences, Calle Nicolás Cabrera, 13-15, Madrid 28049, Spain*
[c] *Department of Statistics and Operations Research, Faculty of Mathematics, Complutense University of Madrid, Madrid 28040, Spain*
[d] *Department of Applied Mathematics, School of Mathematics, University of Leeds, Leeds, LS2 9JT, United Kingdom*

**Abstract**

A stochastic model for the spread of an SIS epidemic among a population consisting of $N$ individuals, each having heterogeneous infectiousness and/or susceptibility, is considered and its behavior is analyzed under the practically relevant situation when $N$ is small. The model is formulated as a finite time-homogeneous continuous-time Markov chain $\mathcal{X}$. Based on an appropriate labeling of states, we first construct its infinitesimal rate matrix by using an iterative argument, and we then present an algorithmic procedure for computing steady-state measures, such as the number of infected individuals, the length of an outbreak, the maximum number of infectives, and the number of infections suffered by a marked individual during an outbreak. The time till the epidemic extinction is characterized as a phase-type random variable when there is no external source of infection, and its Laplace-Stieljtes transform and moments are derived in terms of a forward elimination backward substitution solution. The inverse iteration method is applied to the quasi-stationary distribution of $\mathcal{X}$, which provides a good approximation of the process $\mathcal{X}$ at a certain time, conditional on non-extinction, after a suitable waiting time. The basic reproduction number $\mathcal{R}_0$ is defined here as a random variable, rather than an expected value.

*Keywords:* Basic reproduction number, disease spread, Markov chain model, maximum number of infected individuals, number of infections, outbreak, quasi-stationary regime, stochastic SIS epidemic, heterogeneity

*Corresponding author
*Email addresses:* aeconom@math.uoa.gr (A. Economou), antonio.gomez@icmat.es (A. Gómez-Corral), M.LopezGarcia@leeds.ac.uk (M. López García)
*URL:* http://users.uoa.gr/~aeconom/ (A. Economou), http://icmat.es/antonio.gomez-corral (A. Gómez-Corral), https://www1.maths.leeds.ac.uk/~lopezgarcia/index.html (M. López García)

## 1. Introduction

The SIS model, also known as the contact process, is a simple epidemiological model which has been studied extensively from deterministic and stochastic perspectives under a variety of assumptions; see e.g. the book by Allen [1]. The standard SIS model is a model for the spread of an epidemic among a homogeneously mixed population of $N$ individuals, in which an infective individual becomes susceptible again as soon as its infectious period terminates. Then, in the stochastic version, the standard SIS model is formulated in terms of a finite continuous-time Markov chain (CTMC) $\mathcal{X} = \{X(t) : t \geq 0\}$ where $X(t)$ denotes the number of infectives at time $t$, and its infinitesimal transition probabilities are specified as

$$P\left(X(t+\Delta t) = y \,|X(t) = x\right) \quad = \quad \begin{cases} \frac{\beta}{N} x(N-x)\Delta t + o(\Delta t), & \text{if } y = x+1, \\ \gamma x \Delta t + o(\Delta t), & \text{if } y = x-1, \\ 0, & \text{otherwise,} \end{cases}$$

where $o(\Delta t)/\Delta t \to 0$ as $\Delta t \to 0$. This means that a typical infective makes infectious contacts at the points of a Poisson process with rate $\beta$ during an infectious period, which follows an exponentially distributed recovery time with mean $\gamma^{-1}$, and the individuals contacted at successive contacts are selected independently and uniformly from the $N$ individuals of the population. This uniform mixing (i.e., any infective can infect any susceptible equally easy) becomes more evolved with special structures where either nodes (i.e., individuals) or links may belong to one of a small number of types, thus incorporating heterogeneity in individuals' susceptibility and infectivity. The notions of individuals' susceptibility and infectivity are mainly related to the form and structure of the contact-transmission coefficient $\beta$, when heterogeneities are allowed. For example, a non-uniform mixing is defined by Yates et al. [40], who consider epidemics in heterogeneous populations where individuals are classified in groups; specifically, for groups $i$ and $j$, the infection parameters are given by $\beta_{i,j} = \beta\lambda'_i\pi_{i,j}\mu'_j$, where $\beta$ is some overall measure of infectiousness, $\lambda'_i$ quantifies the infectivity of group $i$ individuals, $\mu'_j$ quantifies the susceptibility of group $j$ individuals, and $\pi_{i,j}$ is a mixing parameter representing the relative preference of group $i$ infective individuals for group $j$ susceptible individuals.

In this paper, the interest is in the stochastic SIS epidemic model, which is formulated here as a finite CTMC allowing us to reflect heterogeneous contacts in terms of disease-causing internal infection rates $\beta_{i,j} \geq 0$. The rates $\beta_{i,j}$ depend on the pair $(i, j)$ as the node $i$ is infected, in such a way that node $j$ becomes infected if it is susceptible and an event of a Poisson process of rate $\beta_{i,j}$ occurs. In addition, disease-causing external rates $\lambda_i \geq 0$ and mean recovery times $\gamma_i^{-1}$ are assumed to depend on node $i$. Unlike the exact $2^N$-state Markov chain analyzed by Van Mieghem et al. [34, Section III], our model with heterogeneous contacts may be thought of as a directed network, that is, a graph in which each edge has a direction, pointing from one node to another in such a way that the adjacency matrix may be asymmetric and disease-causing internal/external infection rates and recovery rates are not necessarily homogeneous.

We refer the reader to the monographs by Newman [23] and Vega-Redondo [36] for a description of theories of processes taking place on networks, such as social networks or search processes on computer networks; as a related work, see also Kephart and White [18]. Directed networks have been used to model epidemics relatively rarely (see e.g. Moslonka-Lefebvre et al. [22] and references therein), but they are relevant to many real-world situations with asymmetries in contact-transmission structures. Keeling and Eames [17] review the basics of epidemiological theory (based on random-mixing models) and network theory (based on work from the social sciences and graph theory), and describe a range of the most popular network types (including random networks, lattices, small-world networks, spatial networks, scale-free networks, and exponential random graph models) and their implications for epidemic spread. Danon et al. [9] provide a personalized overview into the areas of network epidemiology that have seen the greatest progress in recent years, focusing on the types of network relevant to epidemiology, the various ways these networks are characterized, and the analytical approaches and the statistical methods that can be applied to infer the epidemiological parameters on a concrete network. Pautasso et al. [24] focus on small-size directed networks and study the effect of the in- and out-degree of the starting node on the epidemic final size. Recently, Zhang et al. [41] develop an epidemic model for an SIS infection based on semi-directed complex networks, thus extending the scope of previous papers by Meyers et al. [21], and Sharkey et al. [28] to allow for asymmetric contact networks. Wilkinson and Sharkey [39] study Markovian SIS dynamics on finite strongly connected networks, which are applicable to several sexually transmitted diseases and computer viruses, and an exact relationship between invasion probability and (probabilistic) endemic prevalence is proved. In the setting of social networks, Saito et al. [26, 27] consider solving the influence maximization problems on directed networks under the SIS model.

Our major motivation is to analyze various descriptors in the exact $2^N$-state Markov chain model with heterogeneous contacts, and understand the influence of graph characteristics on epidemic spreading under the practically relevant situation when $N$ is small, which is related to small communities sharing confined spaces as families (Brimblecombe et al. [5], Grimwood et al. [14]), nursing homes (Chamchod and Ruan [6]) and intensive care units (ICUs) (Artalejo [3], Austin et al. [4], Cooper et al. [8], Forrester and Pettitt [12], McBryde et al. [20]). The reader is alerted to the fact that our assumption of small population size $N$ does not amount to the term *small-world network* (see e.g. Verdasca et al. [37]), which is described in the work of Watts and Strogatz [38] as an attempt to capture the local nature of transmission and the potential for long-range contacts. Our approach complements and extends previous studies on the SIS type dynamics with heterogeneous contacts. The earlier papers by Simon et al. [29], Van Mieghem et al. [34], and Van Mieghem and Cator [35] focus on undirected graphs where heterogeneities are related to the position of the nodes within the contact network. The descriptor of interest in Simon et al. [29] is the mean transient number of infectives and susceptibles in the contact network. Simon et al. [29] formulate an SIS type model in terms of a CTMC, revisit

lumping and discuss various approximation methods that lead to a significant reduction in the number $2^N - 1$ of equations in the original exact system. For a special class of graphs, they illustrate how the lumped system can be derived by using graph automorphisms. The paper by Taylor et al. [30] builds on the work of Simon et al. [29] and formalizes the link between the SIS type dynamics and the pairwise epidemic model. Van Mieghem and Cator [35] define the $\epsilon$-SIS process by assuming that, besides receiving the infection over links from infected neighbors with rate $\beta$, a node can also get infected by a virus due to some external event with rate $\epsilon$, which was first proposed by Hill et al. [15]. The major advantage of the $\epsilon$-SIS model is that its steady state is different from the overall-healthy state and approximates, for certain small values $\epsilon > 0$, the metastable state, which is characterized by the epidemic threshold. Recently, Sahneh et al. [25] propose a generalized epidemic model, which allows any finite number $M$ of states (susceptible, infective, alert, etc.) per individual and more complex interactions among individuals. More concretely, they deal with a multilayer network that represents the various types of interactions among individuals in such a way that, for example, one layer may model the infection process, while another layer may refer to the dissemination of information that affects their behavior.

In analyzing the underlying CTMC, we present a new labeling of states that, similarly to Simon et al. [29], enables a block-tridiagonal structure for its rate matrix. The block-tridiagonal structure of the rate matrix leads us to a recursive procedure for the construction of its sub-matrices as the population size $N$ increases, and it enables the use of special routines for solving the resulting systems of linear equations in an efficient manner. From a theoretical perspective, our analytical results for the exact $2^N$-state Markov chain model with heterogeneous contacts remain valid regardless of the population size $N$, but at the expense of limited computational tractability. For problems with large networks, Taylor and Kiss [31, Section 2] present a review and summary of the more common approaches to modeling epidemics on networks, including meanfield, pairwise, heterogeneous pairwise, and effective degree model formulations; see also the paper by Gómez et al. [13], who propose a non-perturbative formulation of the heterogeneous mean-field approach in SIS models. For the more general epidemic model introduced by Sahneh et al. [25], the analysis of the exact Markov chain with $M^N$ states is also prohibitive, so the authors propose a mean-field approximation.

The paper is organized as follows. In Section 2, we describe the distributional assumptions that lead us to the exact $2^N$-state Markov chain model with heterogeneous contacts. We first construct the infinitesimal rate matrix of the underlying process $\mathcal{X}$ by using an iterative argument, and then present algorithmic procedures for computing expected extinction times and the quasi-stationary distribution of $\mathcal{X}$ when there is no source of external infection, and various steady-state measures. In Section 3, the interest lies in the length of an outbreak and related measures. We characterize the distribution of the length of an outbreak in terms of a phase-type (PH) random variable, and derive the distribution of the maximum number of individuals that are simultaneously in-

fected, and the distribution of the number of infections suffered by a certain individual during an outbreak. We also replace the role of the basic reproduction number $\mathcal{R}_0$ by the distribution of the exact reproduction number, which has been recently introduced by Artalejo and Lopez-Herrero [2] as a random variable, rather than an expected value. We close, in Section 4, with a few concluding remarks. Some algorithmic solutions and numerical experiments are presented in Appendices C and D.

## 2. Heterogeneous contacts in the stochastic SIS epidemic model

### *2.1. Exact $2^N$-state Markov chain model*

We consider a closed population of $N$ individuals, where each individual passes from being *susceptible* ($S$) to turning *infected* ($I$), to becoming again *susceptible* ($S$), thus allowing for a bidirectional transition between the two possible states. Connections among individuals are described by a connected graph, where the nodes correspond to the individuals, and the edges are their connections, that is, a connection represents a predisposal for a disease-causing contact. We denote the connected graph by $\mathcal{G} = (\mathcal{N}, \mathcal{L})$, where $\mathcal{N} = \{1, 2, ..., N\}$ is the set of nodes, and $\mathcal{L} \subseteq \mathcal{N} \times \mathcal{N}$ is the set of edges, and we associate $\mathcal{G}$ with its adjacency matrix $\mathbf{A} = (a_{i,j} : i, j \in \mathcal{N})$ with $a_{i,j} = 1$ if $(i, j) \in \mathcal{L}$, and 0 if $(i, j) \notin \mathcal{L}$, and the set of neighborhoods $\{\mathcal{N}^i : i \in \mathcal{N}\}$ with $\mathcal{N}^i = \{j : (i, j) \in \mathcal{L}\}$. For each node $i \in \mathcal{N}$, there is an external source of infection, related to nodes that are not represented by $\mathcal{G}$. Disease-causing external infections are assumed to occur according to a Poisson process with rate $\lambda_i \geq 0$ at node $i$. When node $i$ becomes infected, disease-causing internal infections occur according to a Poisson process with rate $\beta_{i,j} > 0$ at every node $j$ with $j \in \mathcal{N}^i$ (i.e., $(i, j) \in \mathcal{L}$), in such a way that node $j$ becomes infected if node $j$ is susceptible and an event of the Poisson process of rate $\beta_{i,j}$ occurs; it is assumed that $\beta_{i,j} = 0$ in the case $j \notin \mathcal{N}^i$ (i.e., $(i, j) \notin \mathcal{L}$). As node $i$ becomes infected, it remains infected for an exponentially distributed time with mean $\gamma_i^{-1} > 0$, and it becomes again susceptible as this exponential infectious (or recovery) period expires. The underlying processes governing disease-causing external/internal infections and recovery times are assumed to be mutually independent.

The state at time $t$ is represented by a vector $\mathbf{X}(t)$ with entries $X_i(t)$ for $i \in \mathcal{N}$, that is, node $i$ is infected (respectively, susceptible) at time $t$, if and only if $X_i(t) = I$ (respectively, $X_i(t) = S$). The process $\mathcal{X} = \{\mathbf{X}(t) = (X_1(t), X_2(t), ..., X_N(t)) : t \geq 0\}$ results in a time-homogeneous CTMC with $2^N$ states. Its state space is denoted by $\mathcal{S} = \{S, I\}^N$. For state $\mathbf{x} \in \mathcal{S}$ and node $j \in \mathcal{N}$, we define vectors $S_j(\mathbf{x})$ and $I_j(\mathbf{x})$ by replacing the $j$th entry of $\mathbf{x}$ by $S$ and $I$, respectively. Then, for states $\mathbf{x}, \mathbf{y} \in \mathcal{S}$, the non-null transition rates of the $2^N$-state process $\mathcal{X}$ are specified by

$$q_{\mathbf{x},\mathbf{y}} = \begin{cases} \lambda_j + \sum_{i \in I(\mathbf{x})} \beta_{i,j}, & \text{if } x_j = S,\ \mathbf{y} = I_j(\mathbf{x}), \\ \gamma_j, & \text{if } x_j = I,\ \mathbf{y} = S_j(\mathbf{x}), \end{cases} \tag{1}$$

and $q_{\mathbf{x}} = -q_{\mathbf{x},\mathbf{x}} = \sum_{j \in S(\mathbf{x})} (\lambda_j + \sum_{i \in I(\mathbf{x})} \beta_{i,j}) + \sum_{j \in I(\mathbf{x})} \gamma_j$, where $x_j$ is the $j$th entry of state $\mathbf{x}$, $I(\mathbf{x}) = \{i \in \mathcal{N} : x_i = I\}$ and $S(\mathbf{x}) = \{i \in \mathcal{N} : x_i = S\}$. Since

the adjacency matrix $\mathbf{A}$ is not assumed to be necessarily symmetric, Equation (1) allows us to reflect heterogeneous contacts, and it can be seen as an elaborate version of Van Mieghem et al. [34, Equation (4)].

We express the state space $\mathcal{S}$ in terms of levels as $\cup_{k=0}^{N} l(k)$, where the $k$th level is given by $l(k) = \{\mathbf{x} \in \mathcal{S} : \#I(\mathbf{x}) = k\}$ for values $k \in \{0, 1, ..., N\}$. If we suppose that states are labeled so that states in $l(k)$ precede those in $l(k+1)$, then the rate matrix $\mathbf{Q}$ of $\mathcal{X}$ has the structured form

$$\mathbf{Q} = \begin{pmatrix} \mathbf{Q}_{0,0} & \mathbf{Q}_{0,1} & & & & \\ \mathbf{Q}_{1,0} & \mathbf{Q}_{1,1} & \mathbf{Q}_{1,2} & & & \\ & \ddots & \ddots & \ddots & & \\ & & \mathbf{Q}_{N-1,N-2} & \mathbf{Q}_{N-1,N-1} & \mathbf{Q}_{N-1,N} \\ & & & \mathbf{Q}_{N,N-1} & \mathbf{Q}_{N,N} \end{pmatrix}, \qquad (2)$$

where $\mathbf{Q}_{k,k'}$ records transition rates related to jumps of $\mathcal{X}$ from states of the $k$th level to states of the $k'$th level, for $k' \in \{k-1, k+1\}$, and $\mathbf{Q}_{k,k}$ is a diagonal matrix of order $\binom{N}{k}$ with entries $-q_{\mathbf{x}}$ for states $\mathbf{x} \in l(k)$. In what follows, we use a matrix formalism; our conventions regarding notation are summarized in Appendix A.

### *2.2. Construction of the rate matrix*

We construct the sub-matrices $\mathbf{Q}_{k,k-1}$ and $\mathbf{Q}_{k,k+1}$ in (2) from their counterparts in a connected graph with $N-1$ nodes. For convenience, let us denote by $\mathbf{Q}_{k,k'}(M)$ the sub-matrix containing transition rates related to jumps from states of the $k$th level to states of the $k'$th level in a connected graph with $M$ nodes; similarly, levels in a connected graph with $M$ nodes are denoted by $l(k|M)$, for values $k \in \{0, 1, ..., M\}$.

By using the reverse lexicographical ordering (Appendix B), it is seen that the level $l(k|M)$, for $1 \leq k \leq M-1$, can be expressed in terms of

$$l(k|M) = l(k|M-1) \times \{S\} \cup l(k-1|M-1) \times \{I\},$$

with $l(0|M) = l(0|M-1) \times \{S\}$ and $l(M|M) = l(M-1|M-1) \times \{I\}$. As a result, sub-matrices $\mathbf{Q}_{k,k-1}(M)$ and $\mathbf{Q}_{k,k+1}(M)$ may be recursively evaluated as follows:

(i) For $k' = k-1$,

$$\begin{aligned} \mathbf{Q}_{1,0}(M) &= \begin{pmatrix} \mathbf{Q}_{1,0}(M-1) \\ \gamma_M \end{pmatrix}, \\ \mathbf{Q}_{k,k-1}(M) &= \begin{pmatrix} \mathbf{Q}_{k,k-1}(M-1) & \mathbf{0}_{\binom{M-1}{k} \times \binom{M-1}{k-2}} \\ \gamma_M \mathbf{I}_{\binom{M-1}{k-1}} & \mathbf{Q}_{k-1,k-2}(M-1) \end{pmatrix}, \quad 2 \leq k \leq M-1, \\ \mathbf{Q}_{M,M-1}(M) &= \begin{pmatrix} \gamma_M, & \mathbf{Q}_{M-1,M-2}(M-1) \end{pmatrix}. \end{aligned}$$

(ii) For $k' = k+1$,

$$\begin{aligned}
\mathbf{Q}_{0,1}(M) &= \left( \mathbf{Q}_{0,1}(M-1),\ \lambda_M \right), \\
\mathbf{Q}_{k,k+1}(M) &= \begin{pmatrix} \mathbf{Q}_{k,k+1}(M-1) & \lambda_M \mathbf{I}_{\binom{M-1}{k}} + \mathbf{U}(k, \beta_{\bullet,M}|M-1) \\ \mathbf{0}_{\binom{M-1}{k-1}\times\binom{M-1}{k+1}} & \mathbf{Q}_{k-1,k}(M-1) + \mathbf{V}(k, \beta_{M,\bullet}|M-1) \end{pmatrix}, \\
& \qquad\qquad 1 \le k \le M-2, \\
\mathbf{Q}_{M-1,M}(M) &= \begin{pmatrix} \lambda_M + \mathbf{U}(M-1, \beta_{\bullet,M}|M-1) \\ \mathbf{Q}_{M-2,M-1}(M-1) + \mathbf{V}(M-1, \beta_{M,\bullet}|M-1)) \end{pmatrix},
\end{aligned}$$

where $\mathbf{U}(k, \beta_{\bullet,M}|M-1)$ is a diagonal matrix of order $\binom{M-1}{k}$ with entries $\sum_{j \in I(\mathbf{x})} \beta_{j,M}$ for every state $\mathbf{x} \in l(k|M-1)$, and the matrix $\mathbf{V}(k, \beta_{M,\bullet}|M-1)$ has dimension $\binom{M-1}{k-1} \times \binom{M-1}{k}$ and non-null entries $\beta_{M,j}$ if $x_j = S$ and $\mathbf{y} = I_j(\mathbf{x})$, for every pair $(\mathbf{x}, \mathbf{y})$ of states with $\mathbf{x} \in l(k-1|M-1)$ and $\mathbf{y} \in l(k|M-1)$. Note that the algorithmic construction of the matrix $\mathbf{Q}_{k-1,k}(M-1) + \mathbf{V}(k, \beta_{M,\bullet}|M-1)$ can be readily implemented by noting that it amounts to the matrix $\mathbf{Q}_{k-1,k}(M-1)$ where each occurrence of rate $\lambda_j$ is replaced by $\lambda_j + \beta_{M,j}$ for $1 \le j \le M-1$.

Therefore, the sub-matrices $\mathbf{Q}_{k,k-1}$ and $\mathbf{Q}_{k,k+1}$ in (2) can be iteratively computed using the aforementioned construction for $1 \le M \le N$, starting with $\mathbf{Q}_{0,1}(1) = (\lambda_1)$ and $\mathbf{Q}_{1,0}(1) = (\gamma_1)$, as $\mathbf{Q}_{k,k-1}(N)$ and $\mathbf{Q}_{k,k+1}(N)$, respectively, and the diagonal elements of $\mathbf{Q}_{k,k}$ are given by the entries of the column vector

$$-\left( (1-\delta_{0,k}) \mathbf{Q}_{k,k-1}(N) \mathbf{1}_{\binom{N}{k-1}} + (1-\delta_{k,N}) \mathbf{Q}_{k,k+1}(N) \mathbf{1}_{\binom{N}{k+1}} \right).$$

The graph of Simon et al. [29], and Van Mieghem et al. [34] amounts to the values $\lambda_i = 0$ and $\gamma_i^{-1} = \gamma^{-1}$ for nodes $i \in \mathcal{N}$, and $\beta_{i,j} = \beta$ if $(i,j) \in \mathcal{L}$, that is, $\beta_{i,j} = 0$ when $i$ and $j$ are not connected by an edge. For this undirected graph, Simon et al. [29] group the $2^N$ states of $\mathcal{S}$ in levels $l(k)$ as in our approach, but they do not specify any concrete labeling for the $\binom{N}{k}$ states of $l(k)$, and they use *lumping* to derive exact models where the number of equations compared to the original system is significantly reduced in such a way that the lumped system is either a reduced but exact version of the original one, or an approximation that in the limit of large graphs ($N \to \infty$) becomes exact. Whilst for graphs with less symmetry the reduction in dimensionality will not be as significant, the original $2^N$-dimensional system in Equation (2) may be lumped to $(N+1)$-, $(2N)$- and $\binom{N/2+3}{3}$-dimensional systems for the complete graph, the star graph, and the household graph, respectively. Van Mieghem and Cator [35] generalize the graph of Simon et al. [29] by adding a nodal component to the infection; i.e., $\lambda_i = \epsilon$ for nodes $i \in \mathcal{N}$, with $\epsilon > 0$. Similarly to Van Mieghem et al. [34], a lexicographical ordering of states leads Van Mieghem and Cator [35] to a bipartite graph and a recursive structure for the rate matrix. However, this ordering does not discriminate the various levels and therefore a nested *fractal-type* structure appears that, though interesting, it cannot be exploited from a computational point of view. In particular, the

bipartite graph does not translate to a recursion for the steady-state vector; see Figures 2 and 3 in Van Mieghem et al. [34] and their related comments. In contrast, our ordering first groups states in levels according to the number of infectives and then arranges them according to the reverse-lexicographic labeling within each level. This enables an efficient construction and economic storage of the rate matrix, as well as the development of stable algorithmic procedures for various epidemic descriptors. In general, the efficient construction of the rate matrix is an important issue of theoretical and practical relevance in epidemics, although it may not be very useful numerically. Sahneh et al. [25, Equations (A6)-(A8)] present such a construction for their generalized model in terms of Kronecker products.

*2.3. The special case $\lambda_i = 0$. Extinction times and quasi-stationary regime*

The assumption $\lambda_i = 0$, for nodes $i \in \mathcal{N}$, turns state $(S, S, ..., S)$ into an absorbing state. In the case of an irreducible class $\mathcal{C} = \cup_{k=1}^{N} l(k)$ of transient states, this means that the epidemic extinction is always certain and the expected times till extinction are all finite, regardless of the initial number of infected nodes. To be concrete, let $T$ be the time till absorption of $\mathcal{X}$, that is, $T = \inf\{t : \mathbf{X}(t) = (S, S, ..., S)\}$. It is then derived that $P(T < \infty | \mathbf{X}(0) = \mathbf{x}) = 1$, and that the expected time $E[T|\mathbf{X}(0) = \mathbf{x}]$ to reach the absorbing state $(S, S, ..., S)$ is finite, for any initial state $\mathbf{x} \in \mathcal{C}$.

Furthermore, the absorption time $T$ can be thought of as a PH random variable with representation $(\tau, \mathbf{Q}^*)$, where $\tau$ is a row vector containing initial probabilities on the class $\mathcal{C}$ of transient states, and the matrix $\mathbf{Q}^*$ is obtained from $\mathbf{Q}$ in (2) by deleting the row and column corresponding to the absorbing state $(S, S, ..., S)$. A direct consequence of this observation is that the cumulative distribution function of $T$ is given by

$$P(T \leq t) \quad = \quad 1 - \tau \exp\{\mathbf{Q}^* t\} \mathbf{1}_{2^N - 1}, \quad t \geq 0.$$

PH distributions can be seen as a natural generalization of the exponential and Erlang distributions; see e.g. Latouche and Ramaswami [19, Chapter 2]. In a general context, a (continuous) PH distribution with representation $(\mathbf{u}, \mathbf{U})$ is defined in terms of the absorption time into state 0 in a CTMC on the state space $\{0, 1, ..., u\}$ with initial probability vector $(u_0, \mathbf{u})$ and infinitesimal generator

$$\begin{pmatrix} 0 & \mathbf{0}_u^T \\ \mathbf{u}_0 & \mathbf{U}^* \end{pmatrix},$$

where $\mathbf{u}$ is a row vector of size $u$, $\mathbf{U}^*$ is a square matrix of order $u$ with entries $(\mathbf{U}^*)_{i,i} < 0$ and $(\mathbf{U}^*)_{i,j} \geq 0$ for $i \neq j$, $u_0 = 1 - \mathbf{u}\mathbf{e}_u$ and $\mathbf{u}_0 = -\mathbf{U}^* \mathbf{e}_u$. In our case, the class $\mathcal{C}$ of transient states amounts to the set $\{1, ..., u\}$, $u = 2^N - 1$, $\mathbf{u} = \tau$ and $\mathbf{U}^* = \mathbf{Q}^*$. To illustrate the modeling appeal of PH random variables, we point out that the family of PH distributions is closed under certain operations such as convolution and convex mixture, and that PH distributions are dense in the class of distributions on $[0, \infty)$. For practical use, the fact that they are associated to Markov processes simplifies conditioning arguments.

The uniformization method (Latouche and Ramaswami [19, Section 2.8]) may be used, in principle, to compute $P(T \leq t)$ for any given $t > 0$. More concretely, we may first uniformize the absorbing CTMC $\mathcal{X}$ with rate matrix $\mathbf{Q}$ by choosing $c = \max\{q_{\mathbf{x}} : x \in \mathcal{S}\}$, and then derive a simple algorithm (Latouche and Ramaswami [19, Figure 2.4]) to compute $P(T \leq t)$ for a fixed value $t > 0$, which might require some caution if $tc$ happens to be large.

We can present an alternative method based on remaining times $T_{\mathbf{x}}$ till epidemic extinction, given that the current state of $\mathcal{X}$ is $\mathbf{x} \in \mathcal{S}$. Consider the Laplace-Stieltjes transforms $\phi(z; \mathbf{x}) = E[e^{-zT_{\mathbf{x}}}]$ for $\mathbf{x} \in \mathcal{C}$ and $Re(z) \geq 0$. For states $\mathbf{x} \in \mathcal{C}$, the Laplace-Stieltjes transforms $\phi(z; \mathbf{x})$ are specified as the unique solution to the set of equations

$$\left( z + \sum_{j \in S(\mathbf{x})} \sum_{i \in I(\mathbf{x})} \beta_{i,j} + \sum_{j \in I(\mathbf{x})} \gamma_j \right) \phi(z; \mathbf{x}) = \sum_{j \in S(\mathbf{x})} \sum_{i \in I(\mathbf{x})} \beta_{i,j} \phi(z; I_j(\mathbf{x})) + \sum_{j \in I(\mathbf{x})} \gamma_j \phi(z; S_j(\mathbf{x})), \quad (3)$$

with $\phi(z; \mathbf{x}) = 1$ if $\mathbf{x} = (S, S, ..., S)$ since $T_{(S,S,...,S)} = 0$ almost surely. In matrix form, Equation (3) becomes

$$\begin{pmatrix} \mathbf{B}_1(z) & \mathbf{C}_1 & & & & \\ \mathbf{A}_2 & \mathbf{B}_2(z) & \mathbf{C}_2 & & & \\ & \ddots & \ddots & \ddots & & \\ & & \mathbf{A}_{N-1} & \mathbf{B}_{N-1}(z) & \mathbf{C}_{N-1} \\ & & & \mathbf{A}_N & \mathbf{B}_N(z) \end{pmatrix} \begin{pmatrix} \phi_1(z) \\ \phi_2(z) \\ \vdots \\ \phi_N(z) \end{pmatrix} = \begin{pmatrix} \mathbf{d}_1 \\ \mathbf{d}_2 \\ \vdots \\ \mathbf{d}_N \end{pmatrix}, \quad (4)$$

where $\phi_k(z)$ is a column vector with entries $\phi(z; \mathbf{x})$ for states $\mathbf{x} \in l(k)$, $\mathbf{A}_k = -\mathbf{Q}_{k,k-1}$ for $2 \leq k \leq N$, $\mathbf{B}_k(z) = z\mathbf{I}_{\binom{N}{k}} - \mathbf{Q}_{k,k}$ for $1 \leq k \leq N$, $\mathbf{C}_k = -\mathbf{Q}_{k,k+1}$ for $1 \leq k \leq N-1$, and $\mathbf{d}_k = \mathbf{Q}_{1,0}$ if $k = 1$, and $\mathbf{0}_{\binom{N}{k}}$ if $2 \leq k \leq N$. Then, we may derive Algorithm 1 (Appendix C.1) for computing the Laplace-Stieltjes transforms $\phi(z; \mathbf{x})$ for states $\mathbf{x} \in \mathcal{C}$. The proof of Algorithm 1 is based on a forward elimination backward substitution solution suggested by Ciarlet [7, page 144].

Let $\phi^{(n)}(\mathbf{x}) = E[T_{\mathbf{x}}^n]$ be the $n$th moment of the infection extinction time, for $n \geq 1$ and state $\mathbf{x} \in \mathcal{S}$, and $\phi_k^{(n)}$ denote the column vector with entries $E[T_{\mathbf{x}}^n]$ for states $\mathbf{x} \in l(k)$ and values $k \in \{0, 1, ..., N\}$; note that $\phi_0^{(n)} = \phi^{(n)}(\mathbf{x}) = 0$ if $\mathbf{x} = (S, S, ..., S)$ and $n \geq 1$. Then, straightforward algebra yields Equation (4) with $\phi_k(z)$ and $\mathbf{B}_k(z)$ replaced by $\phi_k^{(n)}$ and $\mathbf{B}_k(0)$, respectively, and column vectors $\mathbf{d}_k$ replaced by $n\phi_k^{(n-1)}$ for $1 \leq k \leq N$. Algorithm 2 (Appendix C.1) indicates how one may determine the sub-vectors $\phi_k^{(n)}$ in terms of previously computed sub-vectors $\phi_k^{(n-1)}$.

We now turn our attention to the quasi-stationary distribution of $\mathcal{X}$, which provides a good approximation of the distribution of the $2^N$-state process $\mathcal{X}$

at a certain time, conditional on non-extinction, after a suitable waiting time. That is, we examine the limiting behavior of the conditional probabilities

$$P\left(\mathbf{X}(t)=\mathbf{x}\,|\mathbf{X}(0)=\mathbf{x}_0,\mathbf{X}(t)\in\mathcal{C}\right) \quad = \quad \frac{P(\mathbf{X}(t)=\mathbf{x}|\mathbf{X}(0)=\mathbf{x}_0)}{\sum_{\mathbf{z}\in\mathcal{C}}P(\mathbf{X}(t)=\mathbf{z}|\mathbf{X}(0)=\mathbf{x}_0)},$$

for states $\mathbf{x}_0,\mathbf{x}\in\mathcal{C}$, rather than of $P(\mathbf{X}(t)=\mathbf{x}|\mathbf{X}(0)=\mathbf{x}_0)$ itself. For a review of results related to quasi-stationary distributions and two alternative choices (i.e., the *ratio of means* distribution and a *doubly-limiting* conditional distribution) see van Doorn and Pollett [33], and Darroch and Seneta [10, Sections 2 and 4], respectively. In the case of an absorbing CTMC with a single communicating class of transient states, which is our case here, the sub-matrix $\mathbf{Q}^*$ recording transition rates among transient states has all its eigenvalues with negative real parts. Moreover, $\mathbf{Q}^*$ has a unique maximal eigenvalue $-\alpha$, which is real, strictly negative and simple (i.e., its algebraic and geometric multiplicities are both equal to one), and the quasi-stationary distribution of $\mathcal{X}$ is uniquely specified as the left eigenvector $\mathbf{u}$ of $\mathbf{Q}^*$ corresponding to $-\alpha$, with $\mathbf{u}\mathbf{1}_{2^N-1}=1$; see van Doorn and Pollett [33, Theorems 1 and 3].

These observations enable us to determine the quasi-stationary distribution of the $2^N$-state process $\mathcal{X}$ as the unique vector satisfying $\mathbf{u}\mathbf{Q}^*=-\alpha\mathbf{u}$ with $\mathbf{u}\mathbf{1}_{2^N-1}=1$. It is worth noting that we are interested in a single left eigenvector $\mathbf{u}$, corresponding to an eigenvalue $-\alpha$ of a matrix $\mathbf{Q}^*$ of which an approximation $\tilde{\alpha}=0$ is known in advance. Since $\tilde{\alpha}=0$ does not belong to the spectrum of $\mathbf{Q}^*$, we may derive Algorithm 3 (Appendix C.2), which is based on the structured form of the matrix $\mathbf{Q}^*$ and the use of the inverse iteration method (Ciarlet [7, Theorem 6.4-1, exercise 6.4-2]).

*2.4. The case $\sum_{i=1}^{N}\lambda_i>0$. Steady-state measures*

In analyzing the steady-state dynamics of $\mathcal{X}$, we from now on restrict ourselves to an irreducible $2^N$-state process $\mathcal{X}$, and derive its steady-state distribution as the solution to $\pi\mathbf{Q}=\mathbf{0}_{2^N}^T$ with $\pi\mathbf{1}_{2^N}=1$. To begin with, we decompose the vector $\pi$ into sub-vectors $(\pi(0),\pi(1),...,\pi(N))$, where $\pi(k)$ consists of the steady-state probabilities

$$P_{\mathbf{x}} \quad = \quad \lim_{t\to\infty}P(\mathbf{X}(t)=\mathbf{x}|\mathbf{X}(0)=\mathbf{x}_0), \quad \mathbf{x}\in l(k),$$

which do not depend on the initial state $\mathbf{x}_0$ of the process. Algorithm 4 (Appendix C.3) is adapted from Latouche and Ramaswami [19, Chapter 10], and proceeds in two phases. During the first phase, we progressively reduce the state space by removing one level at each step, until we are left with a CTMC on the $N$th level, which is trivially solved since it consists of a single state $\mathbf{x}=(I,I,...,I)$. Then, we construct a normalized steady-state solution in the second phase by adding back one level at each step. The steady-state vector $\pi$ is finally derived by the normalizing equation.

From the above solution, we may compute the steady-state distribution of the number of infected nodes as

$$\lim_{t\to\infty}P(N_{inf}(t)=k) \quad = \quad \pi(k)\mathbf{1}_{\binom{N}{k}}, \quad k\in\{0,1,...,N\},$$

and its corresponding moments; for example, the mean number of nodes that are infected at an arbitrary time is given by $E[N_{inf}] = \sum_{k=1}^{N} k\pi(k)\mathbf{1}_{\binom{N}{k}}$.

Let us assume that, at time $t = 0$, nodes are all susceptible, and define a cycle as the time interval that starts at time $t = 0$ and ends at the first time epoch $t > 0$ at which $\mathbf{X}(t) = (S, S, ..., S)$, after leaving this state. By appealing to the theory of regenerative processes, the steady-state probability $P_{\mathbf{x}}$ can be interpreted as the long-run fraction of time that, during a cycle, the process $\mathcal{X}$ stays in state $\mathbf{x}$, irrespectively of the initial state $\mathbf{x}_0 \in \mathcal{S}$. This means that we may express $P_{\mathbf{x}}$ in terms of mean sojourn times as

$$P_{\mathbf{x}} \quad = \quad (E[L])^{-1} E[L_{\mathbf{x}}],$$

where $L$ is the length of a cycle, and $L_{\mathbf{x}}$ is the amount of time that, during a cycle, the process $\mathcal{X}$ stays in state $\mathbf{x}$. By noting that $P_{\mathbf{x}}$ is the entry of $\pi(k)$ related to state $\mathbf{x}$ if $\mathbf{x} \in l(k)$ with $0 \leq k \leq N$, we have

$$\begin{aligned} E[L] &= \lambda^{-1}\pi^{-1}(0), \\ E[L_{\mathbf{x}}] &= \lambda^{-1}\pi^{-1}(0)P_{\mathbf{x}}, \quad \mathbf{x} \in \mathcal{C}, \end{aligned}$$

with $\lambda = \sum_{i=1}^{N} \lambda_i$. As a result, the expected amount of time that, during a cycle, the number of infected nodes equals $k$ is given by

$$\sum_{\mathbf{x} \in l(k)} E[L_{\mathbf{x}}] \quad = \quad \lambda^{-1}\pi^{-1}(0)\pi(k)\mathbf{1}_{\binom{N}{k}}, \quad 0 \leq k \leq N.$$

## 3. Length of an outbreak and related measures

An outbreak begins when a single node chosen appropriately from the population becomes infected. The disease spreads from the infected node to a neighboring susceptible node at a certain rate, in such a way that each new infected node attempts to infect each of its neighbors and then recovers in accordance with the model description in Section 2.1. The outbreak ends when no infected nodes remain.

Under the assumption of irreducibility, the $2^N$-state process $\mathcal{X}$ will reach the state $(S, S, ..., S)$ starting from any state, meaning that the epidemic always dies out. Let $T'_{\mathbf{x}}$ be the time until the epidemic dies out provided that the process $\mathcal{X}$ currently visits state $\mathbf{x} \in \mathcal{S}$, and $\varphi(z; \mathbf{x})$ be the Laplace-Stieltjes transform $E[e^{-zT'_{\mathbf{x}}}]$, for $Re(z) \geq 0$. It is seen that the sub-vectors $\varphi_k(z)$ with entries $\varphi(z; \mathbf{x})$, for states $\mathbf{x} \in l(k)$ and values $1 \leq k \leq N$, satisfy Equation (4) with $\phi_k(z)$ replaced by $\varphi_k(z)$. However, it should be noted that, unlike Section 2.3 where $\lambda_i = 0$ for every node $i \in \mathcal{N}$, the external infection rates $\lambda_i$ are not necessarily null in the present section. This implies that the Laplace-Stieljtes transforms $E[e^{-zT'_{\mathbf{x}}}]$ and its moments $E[(T'_{\mathbf{x}})^n]$, for states $\mathbf{x} \in \mathcal{C}$ and values $n \geq 1$, can be numerically derived by adapting Algorithms 1 and 2, respectively, and the length $T'_{\mathbf{x}}$ of an outbreak can be thought of as a PH random variable with representation $(\mathbf{e}_{2^N-1}(\mathbf{x}), \mathbf{Q}^*)$.

In what follows, the focus is on three related characteristics allowing us to reflect how the disease spreads on the connected graph $\mathcal{G}$.

*3.1. Maximum values*

Our objective here is to derive the distribution of the maximum level visited by $\mathcal{X}$ (i.e., the maximum number of nodes that are simultaneously infected) during an outbreak, denoted by $N_{max}$.

To evaluate the mass function $P(N_{max} = k|\mathbf{X}(0) = \mathbf{x}_0)$ for values $1 \leq k \leq N$ and initial states $\mathbf{x}_0 \in l(1)$, we modify the $2^N$-state process $\mathcal{X}$ by turning $(S, S, ..., S)$ into an absorbing state, which implies that the set $\mathcal{C} = \cup_{k=1}^{N} l(k)$ becomes an irreducible class of transient states. We may observe that, for $\mathbf{x}_0 \in l(1)$, the conditional probability $P(N_{max} \leq k|\mathbf{X}(0) = \mathbf{x}_0)$ is equal to the probability that, starting from $\mathbf{x}_0$, the process $\mathcal{X}$ enters the absorbing state $(S, S, ..., S)$ but avoiding states of $\cup_{k'=k+1}^{N} l(k')$. Hence, for each fixed $1 \leq k \leq N-1$, we consider an absorbing process $\overline{\mathcal{X}}(k)$ defined on the state space

$$\overline{\mathcal{S}}(k) \quad = \quad \{(S, S, ..., S)\} \cup \bigcup_{k'=1}^{k} l(k') \cup \{k+1\},$$

where state $k+1$ is obtained by lumping the set $\cup_{k'=k+1}^{N} l(k')$ of transient states to make an absorbing state. The rate matrix of $\overline{\mathcal{X}}(k)$ is defined as

$$\overline{\mathbf{Q}}(k) \quad = \quad \begin{pmatrix} 0 & \mathbf{0}_{J(k)}^T & 0 \\ \mathbf{t}_0(k) & \mathbf{T}(k) & \mathbf{t}_{k+1}(k) \\ 0 & \mathbf{0}_{J(k)}^T & 0 \end{pmatrix},$$

where

$$\begin{aligned} \mathbf{t}_0(k) &= \begin{pmatrix} \mathbf{Q}_{1,0} \\ \mathbf{0}_{J'(k)} \end{pmatrix}, \\ \mathbf{T}(k) &= \begin{pmatrix} \mathbf{Q}_{1,1} & \mathbf{Q}_{1,2} & & & \\ \mathbf{Q}_{2,1} & \mathbf{Q}_{2,2} & \mathbf{Q}_{2,3} & & \\ & \ddots & \ddots & \ddots & \\ & & \mathbf{Q}_{k-1,k-2} & \mathbf{Q}_{k-1,k-1} & \mathbf{Q}_{k-1,k} \\ & & & \mathbf{Q}_{k,k-1} & \mathbf{Q}_{k,k} \end{pmatrix}, \qquad (5) \\ \mathbf{t}_{k+1}(k) &= \begin{pmatrix} \mathbf{0}_{J(k-1)} \\ \mathbf{Q}_{k,k+1}\mathbf{1}_{\binom{N}{k+1}} \end{pmatrix}, \end{aligned}$$

with $J(k) = \sum_{k'=1}^{k} \binom{N}{k'}$ and $J'(k) = J(k) - N$. Since the class $\mathcal{C}$ is irreducible, the set $\cup_{k'=1}^{k} l(k')$ consists of communicating transient states and the sub-matrix $\mathbf{T}(k)$ is non-singular. The real part of each eigenvalue of $\mathbf{T}(k)$ is therefore strictly negative and $\mathbf{T}(k)$ is stable. If we expand $\exp\{\mathbf{T}(k)t\}$, and $\mathbf{T}(k)$ is replaced by its Jordan form, then it is also seen that $\lim_{u\to\infty} \exp\{\mathbf{T}(k)u\} = \mathbf{0}_{J(k)\times J(k)}$. We may observe that the column vector

$$\mathbf{p}(k) \quad = \quad \int_0^\infty \exp\{\mathbf{T}(k)u\} du \mathbf{t}_0(k)$$

contains the conditional probabilities that the absorption of $\overline{\mathcal{X}}(k)$ into state $(S, S, ..., S)$ occurs in a finite time. Thus, by noting that the entries of the matrix exponential $\exp\{\mathbf{T}(k)u\}$ amount to the probabilities that up to time $u$ the absorbing process $\overline{\mathcal{X}}(k)$ does not leave the subset $\cup_{k'=1}^{k} l(k')$ of transient states, we notice that the entries of

$$\mathbf{p}(k) \quad = \quad \left(-\mathbf{T}^{-1}(k)\right) \mathbf{t}_0(k)$$

specify the conditional probabilities $P(N_{max} \leq k | \mathbf{X}(0) = \mathbf{x}_0)$ for initial states $\mathbf{x}_0 \in \cup_{k'=1}^{k} l(k')$.

The cumulative distribution function $F_{max}(k) = P(N_{max} \leq k)$ is derived as

$$F_{max}(k) \quad = \quad \sum_{\mathbf{x}_0} P(\mathbf{X}(0) = \mathbf{x}_0) P\left(N_{max} \leq k \,|\mathbf{X}(0) = \mathbf{x}_0\right), \quad 1 \leq k \leq N.$$

Since the first external infection in a completely susceptible population implies an initial state $\mathbf{x}_0 \in l(1)$, the summation above is over $l(1)$. Thus, $F_{max}(k)$ may be expressed in matrix form as

$$F_{max}(k) \quad = \quad \mu(k)\mathbf{p}(k), \quad 1 \leq k \leq N,$$

where $\mu(k)$ has the structured form

$$\mu(k) \quad = \quad \left(\mu(1|k), \mathbf{0}_{J'(k)}\right), \tag{6}$$

and $\mu(1|k)$ consists of initial probabilities over states of level $l(1)$. Note that, in the case $k = N$, we have directly $F_{max}(N) = 1$. We refer the reader to Algorithm 5 (Appendix C.4) for an algorithmic procedure for computing the values $F_{max}(k)$, for $1 \leq k \leq N - 1$.

It should be noted that the sub-vector of initial probabilities in (6) reflects the beginning of an outbreak. In a general setting, a variant of Algorithm 5 can be routinely derived in the case of more than one node initially infected. Specifically, the replacement of $\mu(k)$ in (6) by a vector $(\mu(1|k), \mu(2|k), ..., \mu(k|k))$ of initial probabilities over the subset $\cup_{k'=1}^{k} l(k')$ of transient states, will lead us to compute of $F_{max}(k)$ in terms of $\mu(k)\mathbf{p}(k)$, instead of $\mu(1|k)\mathbf{s}(k)$, in step 3 of Algorithm 5.

### *3.2. Number of infections*

In this section, we characterize the distribution of the number $S'$ of infections suffered by a certain node during an outbreak. For convenience, we focus on the $N$th node. To derive the generating function of the random variable $S'$, we proceed to evaluate in a more general setting the generating functions $\xi(z; \mathbf{x}) = E[z^{S'_{\mathbf{x}}}]$ for $|z| \leq 1$, where $S'_{\mathbf{x}}$ denotes the number of infections suffered by the $N$th node during an interval of length $T'_{\mathbf{x}}$, that is, provided that the current state of the process $\mathcal{X}$ is state $\mathbf{x}$.

Let $\xi_k(z)$ be the column vector containing the generating functions $\xi(z; \mathbf{x})$ for states $\mathbf{x} \in l(k)$ and values $1 \leq k \leq N$. We may observe that $\xi_0(z) = 1$

since $S'_{\mathbf{x}} = 0$ almost surely in the case $\mathbf{x} = (S, S, ..., S)$. For states in $l(k)$ with $1 \leq k \leq N-1$, we partition level $l(k)$ into two sub-levels $l(k;S)$ and $l(k;I)$, where $l(k;S)$ and $l(k;I)$ contain states $\mathbf{x} \in l(k)$ with $x_N = S$ and $x_N = I$, respectively. Sub-levels $l(k;S)$ and $l(k;I)$ enable us to decompose $\xi_k(z)$ into sub-vectors $\xi_k(z;S)$ and $\xi_k(z;I)$, and to reexpress sub-matrices $\mathbf{Q}_{k,k'}$ with $k' \in \{k-1, k, k+1\}$ in (2) as follows:

(i) For $k' = k-1$,

$$\begin{aligned}
\mathbf{Q}_{1,0} &= \begin{pmatrix} \mathbf{Q}_{1,0}(S;S) \\ \gamma_N \end{pmatrix}, \\
\mathbf{Q}_{k,k-1} &= \begin{pmatrix} \mathbf{Q}_{k,k-1}(S;S) & \mathbf{0}_{\binom{N-1}{k}\times\binom{N-1}{k-2}} \\ \gamma_N \mathbf{I}_{\binom{N-1}{k-1}} & \mathbf{Q}_{k,k-1}(I;I) \end{pmatrix}, \quad 2 \leq k \leq N-1, \\
\mathbf{Q}_{N,N-1} &= (\gamma_N, \mathbf{Q}_{N,N-1}(I;I)).
\end{aligned}$$

(ii) For $k' = k$,

$$\begin{aligned}
\mathbf{Q}_{0,0} &= \mathbf{Q}_{0,0}(S;S), \\
\mathbf{Q}_{k,k} &= \mathrm{diag}\left(\mathbf{Q}_{k,k}(S;S), \mathbf{Q}_{k,k}(I;I)\right), \quad 1 \leq k \leq N-1, \\
\mathbf{Q}_{N,N} &= \mathbf{Q}_{N,N}(I;I).
\end{aligned}$$

(iii) For $k' = k+1$,

$$\begin{aligned}
\mathbf{Q}_{0,1} &= \left(\mathbf{Q}_{0,1}(S;S), \mathbf{Q}_{0,1}(S;I)\right), \\
\mathbf{Q}_{k,k+1} &= \begin{pmatrix} \mathbf{Q}_{k,k+1}(S;S) & \mathbf{Q}_{k,k+1}(S;I) \\ \mathbf{0}_{\binom{N-1}{k-1}\times\binom{N-1}{k+1}} & \mathbf{Q}_{k,k+1}(I;I) \end{pmatrix}, \quad 1 \leq k \leq N-2, \\
\mathbf{Q}_{N-1,N} &= \begin{pmatrix} \mathbf{Q}_{N-1,N}(S;I) \\ \mathbf{Q}_{N-1,N}(I;I) \end{pmatrix}.
\end{aligned}$$

We recall that the sub-matrices $\mathbf{Q}_{k,k'}(K;K')$, for $k' \in \{k-1, k+1\}$ and $K, K' \in \{S, I\}$, were derived in Section 2.2 from sub-matrices associated with a connected graph with $N-1$ nodes. For instance, the sub-matrix $\mathbf{Q}_{k,k+1}(K;K')$ is related to a new infection, and $K$ and $K'$ determine states of node $N$ immediately before and after its occurrence; in the case $K = K' = I$ and $1 \leq k \leq N-1$, it has the form

$$\mathbf{Q}_{k,k+1}(I;I) = \mathbf{Q}_{k-1,k}(N-1) + \mathbf{V}(k, \beta_{N,\bullet}|N-1), \tag{7}$$

where non-null entries of $\mathbf{V}(k, \beta_{N,\bullet}|N-1)$ are associated with infections generated only by node $N$; other infections are registered in $\mathbf{Q}_{k-1,k}(N-1)$.

By conditioning on the first transition, we have

(i) For states $\mathbf{x} \in l(k;S)$ with $1 \leq k \leq N-1$,

$$\left(\sum_{j \in S(\mathbf{x})} \left(\lambda_j + \sum_{i \in I(\mathbf{x})} \beta_{i,j}\right) + \sum_{j \in I(\mathbf{x})} \gamma_j\right) \xi(z;\mathbf{x}) = \sum_{j \in I(\mathbf{x})} \gamma_j \xi(z; S_j(\mathbf{x}))$$

$$+\sum_{j\in S(\mathbf{x}),j\neq N}\left(\lambda_j+\sum_{i\in I(\mathbf{x})}\beta_{i,j}\right)\xi(z;I_j(\mathbf{x}))+\left(\lambda_N+\sum_{i\in I(\mathbf{x})}\beta_{i,N}\right)z\xi(z;I_N(\mathbf{x})).$$

(ii) For states $\mathbf{x}\in l(k;I)$ with $1\leq k\leq N$,

$$\left(\sum_{j\in S(\mathbf{x})}\left(\lambda_j+\sum_{i\in I(\mathbf{x})}\beta_{i,j}\right)+\sum_{j\in I(\mathbf{x})}\gamma_j\right)\xi(z;\mathbf{x})=\sum_{j\in I(\mathbf{x})}\gamma_j\xi(z;S_j(\mathbf{x}))$$
$$+\sum_{j\in S(\mathbf{x})}\left(\lambda_j+\sum_{i\in I(\mathbf{x})}\beta_{i,j}\right)\xi(z;I_j(\mathbf{x})).$$

In matrix form, these equations can be written as

$$\begin{aligned}-\mathbf{Q}_{k,k}(S;S)\xi_k(z;S) &= \mathbf{Q}_{k,k-1}(S;S)\xi_{k-1}(z;S)+\mathbf{Q}_{k,k+1}(S;S)\xi_{k+1}(z;S)\\ &\quad+\mathbf{Q}_{k,k+1}(S;I)z\xi_{k+1}(z;I),\quad 1\leq k\leq N-1, \qquad (8)\\ -\mathbf{Q}_{k,k}(I;I)\xi_k(z;I) &= \gamma_N\xi_{k-1}(z;S)+(1-\delta_{1,k})\mathbf{Q}_{k,k-1}(I;I)\xi_{k-1}(z;I)\\ &\quad+(1-\delta_{k,N})\mathbf{Q}_{k,k+1}(I;I)\xi_{k+1}(z;I),\quad 1\leq k\leq N, \qquad (9)\end{aligned}$$

where we denote $\xi_0(z)=\xi_0(z;S)=1$. By (8) and (9), the sub-vectors $\xi_k(z)$, for $1\leq k\leq N$, satisfy Equation (4) with $\mathbf{B}_k(z)$ and $\mathbf{C}_k$ replaced by $\mathbf{B}_k(0)$ and $\mathbf{C}_k(z)$, respectively, where the sub-matrices $\mathbf{C}_k(z)$ are defined by

$$\begin{aligned}\mathbf{C}_k(z) &= -\begin{pmatrix}\mathbf{Q}_{k,k+1}(S;S) & z\mathbf{Q}_{k,k+1}(S;I)\\ \mathbf{0}_{\binom{N-1}{k-1}\times\binom{N-1}{k+1}} & \mathbf{Q}_{k,k+1}(I;I)\end{pmatrix},\quad 1\leq k\leq N-2,\\ \mathbf{C}_{N-1}(z) &= -\begin{pmatrix}z\mathbf{Q}_{N-1,N}(S;I)\\ \mathbf{Q}_{N-1,N}(I;I)\end{pmatrix}.\end{aligned}$$

Thus, by replacing $\mathbf{B}_k(z)$ and $\mathbf{C}_k$ by $\mathbf{B}_k(0)$ and $\mathbf{C}_k(z)$, Algorithm 1 computes the generating functions $\xi(z;\mathbf{x})$ for states $\mathbf{x}\in\mathcal{C}$, and the generating function of the random variable $S'$ can be evaluated as

$$E\left[z^{S'}\right] = \nu(S)\xi_1(z;S)+\nu(I)z\xi_1(z;I),\quad |z|\leq 1,$$

where $\nu(S)$ and $\nu(I)$ record initial probabilities over states in sub-levels $l(1;S)$ and $l(1;I)$, respectively. The amount $\nu(S)\xi_1(0;S)$ represents the probability that node $N$ will not suffer any infection during an outbreak. Similarly, we may evaluate the sub-vectors $\xi_k^{(n)}$ with entries $E[S'_{\mathbf{x}}(S'_{\mathbf{x}}-1)\cdot\ldots\cdot(S'_{\mathbf{x}}-n+1)]$ for states $\mathbf{x}\in l(k)$ and values $1\leq k\leq N$, by replacing the computation of the column vector $\mathbf{w}_k$ at step 2 of Algorithm 2 by

$$\mathbf{w}_k = \mathbf{G}_k^{-1}\left(\mathbf{d}_k+(1-\delta_{1,k})\mathbf{Q}_{k,k-1}\mathbf{w}_{k-1}\right),\quad 1\leq k\leq N-1,$$

with

$$\mathbf{d}_k = \begin{pmatrix}n\mathbf{Q}_{k,k+1}(S;I)\xi_{k+1}^{(n-1)}(I)\\ \mathbf{0}_{\binom{N-1}{k-1}}\end{pmatrix},\quad 1\leq k\leq N-1,$$

and $\mathbf{d}_N = 0$, where $\xi_k^{(n)}(K)$ consists of those entries of $\xi_k^{(n)}$ for states in sub-level $l(k;K)$ with $K \in \{S, I\}$. This leads us to the following expression for the $n$th factorial moment of $S'$

$$E[S'(S'-1)\cdots(S'-n+1)] \quad = \quad \nu(S)\xi_1^{(n)}(S) + \nu(I)\left(\xi_1^{(n)}(I) + n\xi_1^{(n-1)}(I)\right).$$

*3.3. Basic reproduction number*

The basic reproduction number, denoted by $\mathcal{R}_0$, is probably the most important quantity in epidemiology, and it is one of the first descriptors to be estimated during the emergence of a new infectious disease. In the stochastic framework, the role of $\mathcal{R}_0$ is replaced by the distribution of the exact reproduction number $R_{exact,0}$, which has been recently introduced by Artalejo and Lopez-Herrero [2] as a random variable, rather than an expected value. Following to Artalejo and Lopez-Herrero [2, Section 3], we define $R_{exact,0}(i)$ as the exact number of secondary cases generated by node $i$ in the connected graph $\mathcal{G}$ during its entire infectious period.

In this section, we focus on node $N$, and determine the distribution of $R_{exact,0}(N)$ as that of $R'_{(S,\ldots,S,I)}$, where the random variable $R'_{\mathbf{x}}$ records the number of secondary cases generated by node $N$ during its residual infectious period, provided that the current state of $\mathcal{X}$ is $\mathbf{x}$, for states $\mathbf{x} \in l(k;I)$ with $1 \le k \le N$. We first append an extra state, which we denote by $\Delta$, to the subset $\cup_{k=1}^{N} l(k;I)$ of states.

The distribution of $R'_{\mathbf{x}}$, for any state $\mathbf{x} \in l(k;I)$ with $1 \le k \le N$, is inherently connected to a modification of the process $\mathcal{X}$, which is defined on the state space $\{\Delta\} \cup (\cup_{k=1}^{N} l(k;I))$, where $\Delta$ is an absorbing state, and the set $\cup_{k=1}^{N} l(k;I)$ is a class of communicating transient states. The rate matrix of this modified process is given by

$$\begin{pmatrix}
0 & & & & & & \\
\mathbf{q}_1^* & \mathbf{Q}_{1,1}(I;I) & \mathbf{Q}_{1,2}(I;I) & & & & \\
\mathbf{q}_2^* & \mathbf{Q}_{2,1}(I;I) & \mathbf{Q}_{2,2}(I;I) & \mathbf{Q}_{2,3}(I;I) & & & \\
\vdots & & \ddots & \ddots & \ddots & & \\
\mathbf{q}_{N-1}^* & & & \mathbf{Q}_{N-1,N-2}(I;I) & \mathbf{Q}_{N-1,N-1}(I;I) & \mathbf{Q}_{N-1,N}(I;I) \\
\mathbf{q}_N^* & & & & \mathbf{Q}_{N,N-1}(I;I) & \mathbf{Q}_{N,N}(I;I)
\end{pmatrix},$$

where $\mathbf{q}_k^* = \gamma_N \mathbf{1}_{\binom{N-1}{k-1}}$. By using the decomposition formula (7), we have the following equality for the sub-vectors $\psi_k(z)$ with entries $\psi(z;\mathbf{x}) = E\left[z^{R'_{\mathbf{x}}}\right]$, for states $\mathbf{x} \in l(k;I)$ and values $1 \le k \le N$:

$$\begin{aligned}
-\mathbf{Q}_{k,k}(I;I)\psi_k(z) \quad = \quad & \mathbf{q}_k^* + (1-\delta_{1,k})\mathbf{Q}_{k,k-1}(I;I)\psi_{k-1}(z) \\
& + (1-\delta_{k,N})\left(\mathbf{Q}_{k-1,k}(N-1) + z\mathbf{V}(k, \beta_{N,\bullet}|N-1)\right)\psi_{k+1}(z).
\end{aligned}$$

Therefore, sub-vectors $\psi_k(z)$, for $1 \le k \le N$, satisfy (4) with the sub-matrices $\mathbf{A}_k$, $\mathbf{B}_k(z)$, $\mathbf{C}_k$ and $\mathbf{d}_k$ replaced by $-\mathbf{Q}_{k,k-1}(I;I)$, $-\mathbf{Q}_{k,k}(I;I)$, $-(\mathbf{Q}_{k-1,k}(N-1)+z\mathbf{V}(k,\beta_{N,\bullet}|N-1))$ and $\mathbf{q}_k^*$, respectively. We show in Algorithm 6 (Appendix

C.5) how to compute $E\left[z^{R'_{\mathbf{x}}}\right]$, for states $\mathbf{x} \in \cup_{k=1}^{N} l(k;I)$, by adapting our arguments in Algorithm 1.

Sub-vectors $\psi_k^{(n)}$ of factorial moments $E[R'_{\mathbf{x}}(R'_{\mathbf{x}}-1)\cdot ...\cdot (R'_{\mathbf{x}}-n+1)]$, for states $\mathbf{x} \in l(k;I)$ with $1 \leq k \leq N$, can be also evaluated from Algorithm 6 by replacing $\mathbf{C}_k(z)$ and $\mathbf{d}_k$ by $\mathbf{C}_k(1)$ and $(1-\delta_{k,N})n\mathbf{V}(k,\beta_{N,\bullet}|N-1)\psi_{k+1}^{(n-1)}$, respectively. The expected number of secondary infections generated by node $N$, during its entire infectious period, is then determined as $E[R_{exact,0}(N)] = \psi_1^{(1)}$, since $\psi_1(z) = E[z^{R_{exact,0}(N)}]$. A population-based version of this expected value is given by

$$E[R_{exact,0}] \quad = \quad \lambda^{-1}\sum_{i=1}^{N}\lambda_i E[R_{exact,0}(i)],$$

where the term $\lambda^{-1}\lambda_i$ specifies the probability that, in a completely susceptible population, the disease transmission is caused by node $i$.

In Diekmann et al. [11], we may find an interesting discussion on how various indicators of the infectiousness of an individual (such as the basic reproduction number $\mathcal{R}_0$, the speed $c_0$ of the spatial propagation of an infection and the probability of a major outbreak, among others) can be used to describe the spread of an epidemic in a network. The main argument in Diekmann et al. [11, Section 10.6] is that $\mathcal{R}_0$ cannot provide sufficient information for the spread of an epidemic in a general network. In particular, two simple situations are presented, when the individuals of a finite population occupy the positions of an integer lattice on a line, and when they are placed on the nodes of a regular lattice in a plane. In the former case, the possibility of a major outbreak can be characterized in terms of $\mathcal{R}_0$, whereas in the latter it cannot. The reason is that, in a network with loops, there does not exist a *typical* spatial configuration of already infected and still susceptible individuals, unlike in the integer lattice on a line. Thus, $\mathcal{R}_0$ makes sense for networks with a tree configuration, but its value is arguable for more complex network structures.

In contrast to $\mathcal{R}_0$, the exact reproduction number $R_{exact,0}$ does not take into account only the immediate neighbors of an individual, but rather it considers the whole effect of an initially infected individual on the network till its first recovery. Moreover, it takes into account not only the underlying contact structure but also the differences in the levels of susceptibility, infectivity and recovery of an individual. This more detailed information comes at a higher computational cost, which is not prohibitive for small populations. The computation of $R_{exact,0}$ (or its first moment) when $N$ is small can help to shed light on various natural questions. For example, in the case of a newly infected family (Appendix D), it may answer to questions like 'Does the nature of the first infected member (child, mother, father) influence the number of members that will be affected till the first recovery?' or 'How many members will be affected till the recovery of the first infected member?'

## 4. Discussion

In this paper, we describe the network of contacts between individuals by a graph $\mathcal{G} = (\mathcal{N}, \mathcal{L})$ with members of the population represented by nodes in $\mathcal{N}$, and with connections between individuals represented by edges in $\mathcal{L}$. The $2^N$-state process $\mathcal{X}$ amounts to a directed graph $\mathcal{G}$, whence we complement and extend previous studies (Simon et al. [29], Van Mieghem et al. [34], Van Mieghem and Cator [35]) where the authors treat undirected networks, with disease transmission possible in either direction along an edge.

A key idea in the paper is an appropriate labeling of states in $\mathcal{S}$, which differs from the lexicographic ordering assumed by Van Mieghem et al. [34], and Van Mieghem and Cator [35]. Similarly to Simon et al. [29], we group the $2^N$ states of $\mathcal{S}$ in levels $l(k)$ according to the number $k \in \{0, 1, ..., N\}$ of infectives, which leads to a block-tridiagonal rate matrix $\mathbf{Q}$ in (2). In addition, we use a reverse-lexicographic labeling of states in level $l(k)$ and, for a population of $N$ individuals, we construct the sub-matrices $\mathbf{Q}_{k,k-1}$ and $\mathbf{Q}_{k,k+1}$ in (2) in terms of their counterparts for $N-1$ individuals. The iterative construction in Section 2.2 enables a more economic storage of the infinitesimal transition rates, as well as the use of special routines for solving the resulting systems of linear equations for the various epidemic descriptors in Sections 2.3, 2.4 and 3.

The existing literature on epidemic models on networks is essentially focussed on phase-transition phenomena (critical thresholds, which are linked to a major outbreak), the transient distribution and some related distributions (metastable state) of the number of infectives. Our interest is in epidemic descriptors that quantify the spread of the epidemic at a population level (steady-state measures, extinction times, quasi-stationary regime, and maximum values), and at an individual level (number of infections during an outbreak, and number of secondary cases generated by a certain individual). In studying descriptors, our labeling of states plays a crucial role when defining suitable absorbing versions of the process $\mathcal{X}$, and adapting well-known numerically stable solutions (block-Gaussian elimination, inverse iteration method, etc.) for their efficient implementation. It is not clear how these descriptors could be investigated with the previously proposed orderings of states.

Whilst we show how current SIS type models can be extended in a way that captures a variety of network topologies and heterogeneities in individuals' infectiousness and susceptibility, the analytical treatment of the exact $2^N$-state Markov chain will have a more theoretical rather than practical motivation in the case of network sizes $N \geq 20$. In Appendix D, the approach is seen to perform well with regard to both accuracy and speed for networks with sizes $N \leq 15$ and a variety of configurations. Table 1 briefly summarizes a preliminary set of numerical experiments for a complete graph with uniform mixing (Van Mieghem and Cator [35]), and it shows that the steady-state vector of the process $\mathcal{X}$ can be more efficiently evaluated with Algorithm 4 than with general-purpose algorithms. Differences in execution times become more apparent with increasing population sizes $N$. This is mainly explained by the fact that, in solving numerically the $2^N$-dimensional system $\pi\mathbf{Q} = \mathbf{0}_{2^N}^T$ with $\pi\mathbf{1}_{2^N} = 1$, the

Table 1: Execution times in computing the mean number $E[N_{inf}]$ of infectives for the graph of Van Mieghem and Cator [35] with $\epsilon = 2.0$, $\beta = 2.0$ and $\gamma = 4.0$.

| $N$ | 10 | 11 | 12 | 13 | 14 | 15 | 16 | 17 |
|---|---|---|---|---|---|---|---|---|
| LU factorization | 0.19s | 1.38s | 9.91s | 1m14.22s | 10m14.53s | 1h15m36.41s | — | — |
| Algorithm 4 | 0.02s | 0.13s | 0.77s | 5.41s | 45.63s | 4m59.94s | 1h22m24.76s | 10h45m1.97s |

approach leads us to solve $N+1$ systems of linear equations for $\binom{N}{k}$ unknowns, with $k \in \{0, 1, ..., N\}$, which reduces significantly the computational burden for a fixed size $N$. The uniform mixing in the complete graph is considered in Table 1 not for any computational convenience, but for testing the accuracy by noting that the uniform mixing in the complete graph yields a birth-and-death process governing the process $\mathcal{X}$ in steady-state. In evaluating numerical results, we use the Python programming language in a high performance computing facility – quad-core AMD 8384 (2.7Ghz) processor with 64GB of DDR2 memory – of the University of Leeds.

It is clear that, from a practical point of view, the increase in the range of $N$ for which Algorithm 4 provides a numerical solution, while conventional tools cannot, is not qualitatively significant in our examples (Table 1). However, from a theoretical perspective, the ordering of states and the recursive construction of the rate matrix in Sections 2.1 and 2.2 are neat, and they provide a path for the study of epidemic descriptors that have not been considered earlier.

The main idea that relies in the ordering of states (Sections 2.1 and 2.2) can be extended in more general epidemic models with multiple individual states or compartments, which would yield a state space $\mathcal{S}$ structured by levels and sub-levels. For example, a similar analysis can be carried out for SIR type models, where susceptible individuals become infected, and infected individuals eventually become recovered, staying in this state for the rest of the process. In this case, we may express $\mathcal{S}$ in terms of levels as

$$\mathcal{S} \quad = \quad \bigcup_{k=0}^{N} l(k). \tag{10}$$

The $k$th level is now given by $l(k) = \cup_{i=0}^{N-k} l'(k;i)$, and the sub-levels are defined by $l'(k;i) = \{\mathbf{x} \in \mathcal{S} : \#R(\mathbf{x}) = k, \#I(\mathbf{x}) = i\}$, where $\#R(\mathbf{x})$ and $\#I(\mathbf{x})$ denote the numbers of recovered and infected individuals in state $\mathbf{x}$, respectively. For practical use, our algorithmic solution and the Kronecker's products approach in Sahneh et al. [25] will fail for moderate values of $N$, since $\#\mathcal{S} = 3^N$ in the SIR type model; similarly to the SIS model, the labeling of states in (10) permits to study various descriptors, such as the duration of an outbreak, the final size of the epidemic, and the number of simultaneously infected individuals during an outbreak. Unlike the block-tridiagonal structure of $\mathbf{Q}$ in the SIS model, Equation (10) yields a rate matrix with a special block-bidiagonal structure. The numerical relevance of this statement is that, in studying these descriptors, no inverses are needed to be computed in the resulting algorithmic procedures

and, consequently, efficient recursions can be obtained.

*Acknowledgements*

We thank the referees for their careful consideration of our paper and their constructive comments. Financial support for this work was provided by the Government of Spain (Ministry of Economy and Competitiveness) and the European Commission through the project MTM-2011-23864 and the grant BES-2009-018747.

## Appendix A. Glossary of notation

For ease of reference we summarize here some of the notation that is used in the rest of paper.

Matrices have uppercase and vectors lowercase letters. The transpose of $\mathbf{W}$ is written as $\mathbf{W}^T$. For a square matrix $\mathbf{W}$, the matrix exponential is defined by $\exp\{\mathbf{W}\} = \sum_{n=0}^{\infty}(n!)^{-1}\mathbf{W}^n$. We denote by $\mathbf{I}_a$ and $\mathbf{0}_{a\times b}$ the identity matrix of order $a$ and the null matrix of dimension $a \times b$, respectively. The matrix $\text{diag}(e_1, ..., e_a)$ is the square matrix having elements $e_1$, ..., $e_a$ along its diagonal and zeros elsewhere, even if the entries $e_1$, ..., $e_a$ are matrices.

We let $\mathbf{1}_a$ be the column vector of order $a$ of 1s, and $\mathbf{0}_a$ be the column vector of order $a$ of 0s. The vector $\mathbf{e}_a(\mathbf{x})$ is a column vector of order $a$ such that all entries equal zero, with the exception of the entry for state $\mathbf{x}$ which is equal to one. Finally, $\delta_{a,b}$ denotes Kronecker's delta, and $\#\mathcal{B}$ denotes cardinality of a set $\mathcal{B}$.

## Appendix B. Reverse lexicographical ordering

For states of level $l(k)$ in the connected graph $\mathcal{G}$, the reverse lexicographical ordering is derived as follows. First, states $\mathbf{x} \in \mathcal{S}$ are translated into states $\mathbf{x} \in \{0,1\}^N$ by replacing $S$ and $I$ by 0 and 1, respectively. Second, resulting states $\mathbf{x} \in \{0,1\}^N$ within level $l(k)$ are ordered by using the lexicographical ordering. Third, states in the form $(x_1, x_2, ..., x_N)$ with entries $x_i \in \{0,1\}$ are then rewritten as states $(x_N, x_{N-1}, ..., x_1)$ with $x_i \in \{S, I\}$.

As an example, we consider the case $N = 4$ and $k = 2$. This gives a total of six states, which are ordered as $(0,0,1,1) \prec (0,1,0,1) \prec (0,1,1,0) \prec (1,0,0,1) \prec (1,0,1,0) \prec (1,1,0,0)$. States in $l(2)$ are then ordered as

$$(I,I,S,S) \prec (I,S,I,S) \prec (S,I,I,S) \prec (I,S,S,I) \prec (S,I,S,I) \prec (S,S,I,I).$$

## Appendix C. Algorithmic solutions

### *Appendix C.1. Algorithms 1 and 2*

Algorithms 1 and 2 provide iterative procedures for computing the Laplace-Stieltjes transforms $\phi(z;\mathbf{x})$ in (4), and their moments $E[T_{\mathbf{x}}^n]$, for states $\mathbf{x} \in \mathcal{C}$ and $n \geq 1$.

**Algorithm 1** Computation of $E[e^{-zT_{\mathbf{x}}}]$ for states $\mathbf{x} \in \mathcal{C}$

*Step 1:* $k := 1$;
$\mathbf{G}_k(z) := z\mathbf{I}_N - \mathbf{Q}_{1,1}$;
$\mathbf{w}_k(z) := \mathbf{G}_1^{-1}(z)\mathbf{Q}_{1,0}$;
while $k < N$, repeat
$k := k + 1$;
$\mathbf{G}_k(z) := z\mathbf{I}_{\binom{N}{k}} - \mathbf{Q}_{k,k} - \mathbf{Q}_{k,k-1}\mathbf{G}_{k-1}^{-1}(z)\mathbf{Q}_{k-1,k}$;
$\mathbf{w}_k(z) := \mathbf{G}_k^{-1}(z)\mathbf{Q}_{k,k-1}\mathbf{w}_{k-1}(z)$.
*Step 2:* $\phi_k(z) := \mathbf{w}_k(z)$;
while $k > 1$, repeat
$k := k - 1$;
$\phi_k(z) := \mathbf{w}_k(z) + \mathbf{G}_k^{-1}(z)\mathbf{Q}_{k,k+1}\phi_{k+1}(z)$.

**Algorithm 2** Computation of $E[T_{\mathbf{x}}^n]$ for states $\mathbf{x} \in \mathcal{C}$ and $n \geq 1$

*Step 1:* $k := 1$;
$\mathbf{G}_k := -\mathbf{Q}_{1,1}$;
$\mathbf{w}_k := n\mathbf{G}_k^{-1}\phi_k^{(n-1)}$;
while $k < N$, repeat
$k := k + 1$;
$\mathbf{G}_k := -\mathbf{Q}_{k,k} - \mathbf{Q}_{k,k-1}\mathbf{G}_{k-1}^{-1}\mathbf{Q}_{k-1,k}$;
$\mathbf{w}_k := \mathbf{G}_k^{-1}(n\phi_k^{(n-1)} + \mathbf{Q}_{k,k-1}\mathbf{w}_{k-1})$.
*Step 2:* $\phi_k^{(n)} := \mathbf{w}_k$;
while $k > 1$, repeat
$k := k - 1$;
$\phi_k^{(n)} := \mathbf{w}_k + \mathbf{G}_k^{-1}\mathbf{Q}_{k,k+1}\phi_{k+1}^{(n)}$.

Algorithms 1 and 2 lead themselves to stable computations since $\mathbf{G}_k(z)$ has non-positive off-diagonal elements and strictly positive row sums for $Re(z) \geq 0$, and $\mathbf{G}_k = \mathbf{G}_k(0)$. More particularly, the value

$$z + \sum_{i \in I(\mathbf{x})} \sum_{j \in S(\mathbf{x})} \beta_{i,j}$$

results in a lower bound to the row sum corresponding to state $\mathbf{x} \in l(k)$, which implies that the matrix $\mathbf{G}_k(z)$ is nonsingular, for $Re(z) \geq 0$. Elements of $\mathbf{G}_k^{-1}(z)$ are thus nonnegative; see Latouche and Ramaswami [19, Theorem 2.4.3].

*Appendix C.2. Algorithm 3*

Steps 1 and 2 in Algorithm 3 show how, in a specialized manner, one proceeds when solving $\mathbf{u}_{k'+1}\mathbf{Q}^* = \mathbf{u}_{k'}$ by block-Gaussian elimination.

**Algorithm 3** Computation of the quasi-stationary distribution of $\mathcal{X}$

*Step 1:* $k' := 0$;
$k := N$;
$\mathbf{Q}_k^* := \mathbf{Q}_{N,N}$;
select $\mathbf{u}_{k'} := (\mathbf{u}_0(1), \mathbf{u}_0(2), ..., \mathbf{u}_0(N))$;
while $k > 1$, repeat
$k := k - 1$;
$\mathbf{Q}_k^* := \mathbf{Q}_{k,k} + \mathbf{Q}_{k,k+1}(-\mathbf{Q}_{k+1}^*)^{-1}\mathbf{Q}_{k+1,k}$;
while $k < N - 2$, repeat
$\mathbf{R}_k := \mathbf{Q}_{k,k+1}(-\mathbf{Q}_{k+1}^*)^{-1}$;
$\mathbf{G}_k := (-\mathbf{Q}_{k+1}^*)^{-1}\mathbf{Q}_{k+1,k}$;
$k := k + 1$.
*Step 2:* $k := N$;
$\mathbf{v}_{k'+1}(k) := \mathbf{u}_{k'}(N)$;
while $k > 1$, repeat
$k := k - 1$;
$\mathbf{v}_{k'+1}(k) := \mathbf{u}_{k'}(k) + \mathbf{v}_{k'+1}(k+1)\mathbf{G}_k$;
$\mathbf{u}_{k'+1}(1) := \mathbf{v}_{k'+1}(1)(\mathbf{Q}_1^*)^{-1}$;
while $k < N - 1$, repeat
$k := k + 1$;
$\mathbf{u}_{k'+1}(k) := \mathbf{v}_{k'+1}(k)(\mathbf{Q}_k^*)^{-1} + \mathbf{u}_{k'+1}(k-1)\mathbf{R}_{k-1}$.
*Step 3:* If $||\mathbf{u}_{k'+1} - \mathbf{u}_{k'}|| > \varepsilon$, then
$k' := k' + 1$;
repeat step 2;
else
$\mathbf{u} := (\mathbf{u}_{k'+1}\mathbf{1}_{2^N-1})^{-1}\mathbf{u}_{k'+1}$;
endif.

For practical use, we shall select $\mathbf{u}_0$ as an arbitrary non-zero vector (Ciarlet [7, page 213]) but we point out that, from a theoretical perspective, it corresponds to a vector that does not belong to the subspace spanned by the vectors corresponding to the eigenvalues which are distinct from $-\alpha$. Step 3 will progressively increase $k'$ until finding a suitable approximation to the limit

$$\lim_{k' \to \infty} (-1)^{k'} \left(||\mathbf{u}_{k'}||\right)^{-1} \mathbf{u}_{k'} \quad = \quad \mathbf{u},$$

with a predetermined accuracy $\varepsilon > 0$, which holds true regardless of the vector norm $||\cdot||$ under consideration.

*Appendix C.3. Algorithm 4*

Here is an algorithmic procedure for computing the steady-state distribution of the $2^N$-state process $\mathcal{X}$.

**Algorithm 4** Computation of the steady-state distribution of $\mathcal{X}$

*Step 1:* $k := 0$;

$\mathbf{Q}_k^* := \mathbf{Q}_{0,0}$;
while $k < N-2$, repeat
$k := k+1$;
$\mathbf{Q}_k^* := \mathbf{Q}_{k,k} + \mathbf{Q}_{k,k-1}(-\mathbf{Q}_{k-1}^*)^{-1}\mathbf{Q}_{k-1,k}$.

*Step 2:* $k := N$;
$\pi^*(k) := 1$;
while $k > 0$, repeat
$k := k-1$;
$\pi^*(k) := \pi^*(k+1)\mathbf{Q}_{k+1,k}(-\mathbf{Q}_k^*)^{-1}$.

*Step 3:* $k := N$;
$\pi(k) := \left(1 + \sum_{k'=0}^{N-1} \pi^*(k')\mathbf{1}_{\binom{N}{k'}}\right)^{-1}$;
while $k > 0$, repeat
$k := k-1$;
$\pi(k) := \pi(N)\pi^*(k)$.

*Appendix C.4. Algorithm 5*

Algorithm 5 is inspired from block-Gaussian elimination, and it is based on the partition of $\mathbf{T}(k)$ into sub-matrices

$$\mathbf{T}(k) \quad = \quad \begin{pmatrix} \mathbf{T}(k-1) & \mathbf{C}'_{1,2}(k-1) \\ \mathbf{C}'_{2,1}(k-1) & \mathbf{Q}_{k,k} \end{pmatrix},$$

where $\mathbf{C}'_{1,2}(k-1)$ and $\mathbf{C}'_{2,1}(k-1)$ are defined from (5) in an appropriate manner. Sub-matrices $\mathbf{C}_{1,2}(k-1)$ and $\mathbf{C}_{2,2}(k-1)$ in step 2 are then obtained by evaluating $-\mathbf{T}^{-1}(k)$ from Hunter [16, Theorem 4.2.4].

**Algorithm 5** Computation of $F_{max}(k)$

*Step 1:* $k := 1$;
$\mathbf{C}_{2,2}(k) := -\mathbf{Q}_{1,1}^{-1}$;
$\mathbf{p}(k) := \left(\left(\sum_{j=1,j\neq k'}^{N}(\lambda_j + \beta_{k',j}) + \gamma_{k'}\right)^{-1}\gamma_{k'} : 1 \leq k' \leq N\right)$;
$\mathbf{p}_1(k) := \mathbf{p}(k)$.

*Step 2:* While $k < N-1$, repeat
$k := k+1$;
$\mathbf{C}_{2,2}(k) := -\left(\mathbf{Q}_{k,k} + \mathbf{Q}_{k,k-1}\mathbf{C}_{2,2}(k-1)\mathbf{Q}_{k-1,k}\right)^{-1}$;
if $k = 2$, then
$\mathbf{p}_{\leq k-1}(k) := \mathbf{C}_{2,2}(k-1)\mathbf{Q}_{k-1,k}\mathbf{C}_{2,2}(k)\mathbf{Q}_{k,k-1}\mathbf{p}_{k-1}(k-1)$,
$\mathbf{p}_{\leq k-1}(k) := \mathbf{p}_{k-1}(k-1) + \mathbf{p}_{\leq k-1}(k)$,
else
$\mathbf{p}_{\leq k-1}(k) := \begin{pmatrix} \mathbf{C}_{1,2}(k-1)\mathbf{Q}_{k-1,k}\mathbf{C}_{2,2}(k)\mathbf{Q}_{k,k-1}\mathbf{p}_{k-1}(k-1) \\ \mathbf{C}_{2,2}(k-1)\mathbf{Q}_{k-1,k}\mathbf{C}_{2,2}(k)\mathbf{Q}_{k,k-1}\mathbf{p}_{k-1}(k-1) \end{pmatrix}$,
$\mathbf{p}_{\leq k-1}(k) := \begin{pmatrix} \mathbf{p}_{\leq k-2}(k-1) \\ \mathbf{p}_{k-1}(k-1) \end{pmatrix} + \mathbf{p}_{\leq k-1}(k)$,
endif;

$\mathbf{C}_{1,2}(k) := \begin{pmatrix} \mathbf{C}_{1,2}(k-1)\mathbf{Q}_{k-1,k}\mathbf{C}_{2,2}(k) \\ \mathbf{C}_{2,2}(k-1)\mathbf{Q}_{k-1,k}\mathbf{C}_{2,2}(k) \end{pmatrix}$;
$\mathbf{p}_k(k) := \mathbf{C}_{2,2}(k)\mathbf{Q}_{k,k-1}\mathbf{p}_{k-1}(k-1)$;
$\mathbf{p}(k) := \begin{pmatrix} \mathbf{p}_{\leq k-1}(k) \\ \mathbf{p}_k(k) \end{pmatrix}$;
$\mathbf{s}(k) := ((\mathbf{p}(k))_{k'} : 1 \leq k' \leq N)$.

*Step 3:* $F_{max}(k) := 1$;
while $k > 1$, repeat
$k := k - 1$;
$F_{max}(k) := \mu(1|k)\mathbf{s}(k)$.

*Appendix C.5. Algorithm 6*

By adapting Algorithm 1, we derive the following procedure for evaluating $E\left[z^{R'_{\mathbf{x}}}\right]$, for states $\mathbf{x} \in \cup_{k=1}^{N} l(k;I)$:

**Algorithm 6** Computation of $E\left[z^{R'_{\mathbf{x}}}\right]$ for states $\mathbf{x} \in \cup_{k=1}^{N} l(k;I)$

*Step 1:* $k := 0$;
while $k < N-2$, repeat
$k := k + 1$;
$\mathbf{G}_k(z) := -\mathbf{Q}_{k,k}(I;I) + (1-\delta_{1,k})\mathbf{Q}_{k,k-1}(I;I)\mathbf{G}_{k-1}^{-1}(z)\mathbf{C}_{k-1}(z)$;
$\mathbf{w}_k(z) := \mathbf{G}_k^{-1}(z)\left(\mathbf{d}_k + (1-\delta_{1,k})\mathbf{Q}_{k,k-1}(I;I)\mathbf{w}_{k-1}(z)\right)$.

*Step 2:* $k := N$;
$\psi_k(z) := \left(-\mathbf{Q}_{N,N}(I;I) + \mathbf{Q}_{N,N-1}(I;I)\mathbf{G}_{N-1}^{-1}(z)\mathbf{C}_{N-1}(z)\right)^{-1}$;
$\psi_k(z) := \psi_k(z)(\mathbf{q}_N^* + \mathbf{Q}_{N,N-1}(I;I)\mathbf{w}_{N-1}(z))$;
while $k > 1$, repeat
$k := k - 1$;
$\psi_k(z) := \mathbf{w}_k(z) - \mathbf{G}_k^{-1}(z)\mathbf{C}_k(z)\psi_{k+1}(z)$.

## Appendix D. Numerical experiments

In this appendix, our numerical work is related to the spread of the syndrome *Acute coryza* within a family, and infections caused by nosocomial pathogens in an intensive care unit. Supplementary material related to numerical experiments can be found online at `http://dx.doi.org/10.1016/j.physa.***`. Throughout this section, we use here the notation $T'$ and $S'$ instead of $T'_{\mathbf{x}}$ and $S'_{\mathbf{x}}$ as the initial infective $\mathbf{x}$ is well specified by the context.

*Appendix D.1. On the spread of Acute coryza among five-member families*

In this example, results are related to a classical study conducted by Brimblecombe et al. [5], which is designed to describe the introduction and spread of respiratory diseases among families of the same size and structure living in the same district at the same time, but under varying domestic conditions. Specifically, our interest is in the syndrome *Acute coriza*. In the survey by Brimblecombe et al. [5], only families consisting of father, mother and three

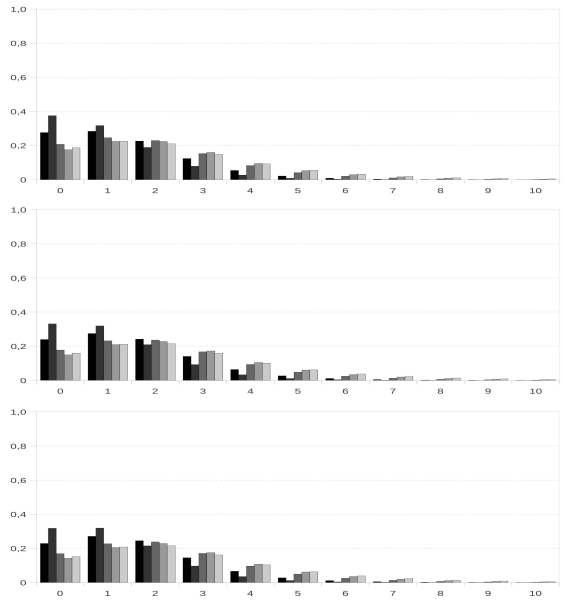


Figure D.1: Mass function of $R_{exact,0}$ for (*from top to bottom*) uncrowded, crowded and overcrowded families, when the tagged individual corresponds (*from left to right*) to the father, the mother, the oldest child, the middle child and the youngest child.

children (of whom one was under 5 years of age) are included. These families live in a separate and independent household with their own living and sleeping accommodation, whether in their own house, self-contained flat, or tenement accommodation, and they are monitored during two years. The information obtained is of two kinds: (i) basic data concerning the environment of the family and of their health before the survey is begun; and (ii) serial data concerning the clinical infections and bacteriological findings encountered during the course of the survey. To reflect that infection is transferred more readily in the more crowded homes, the families are divided into three groups: *uncrowded*, *crowded* and *overcrowded*, in such a way that the degree of crowding is assessed from the number of rooms available. The individuals in the survey are classified in five types: father, mother, oldest child (termed *child 1*), middle child (*child 2*), and youngest child (*child 3*); in particular, the oldest and middle children are school-children, and the youngest one is a pre-school-child.

For each type of housing condition, the study yields several statistics concerning with the introduction and secondary attack rates of *Acute coryza* [5, Table III]. For each type of individual, the study gives statistics related to the introduction and secondary attack rates of *Acute coryza* [5, Table IV], the cross-infection rates [5, Table V], and the ratios quantifying the relative susceptibility and the relative communicability [5, Table VI]. Based on this set of empirical data in [5], we specify a stochastic SIS epidemic model with five nodes, each having heterogeneous infectiousness and/or susceptibility. Concrete specifica-

Table D.2: Mean length $E[T']$ of an outbreak, mean number $E[N_{inf}]$ of infected individuals in steady state, and mean exact reproduction number $E[R_{exact,0}]$ versus housing conditions.

| | Initial infective | Uncrowded | Crowded | Overcrowded |
|---|---|---|---|---|
| $E[T']$ | Father | 13.50112 | 21.62513 | 25.26581 |
| | Mother | 11.72094 | 19.03885 | 22.35284 |
| | Child 1 | 15.19095 | 23.89612 | 27.76915 |
| | Child 2 | 15.94390 | 24.87605 | 28.84198 |
| | Child 3 | 15.77180 | 24.59425 | 28.51996 |
| $E[N_{inf}]$ | | 1.11696 | 1.53312 | 1.83873 |
| $E[R_{exact,0}]$ | Father | 1.52631 | 1.67343 | 1.71588 |
| | Mother | 1.10959 | 1.23341 | 1.26964 |
| | Child 1 | 1.97870 | 2.14887 | 2.19760 |
| | Child 2 | 2.28243 | 2.46109 | 2.51139 |
| | Child 3 | 2.34125 | 2.53071 | 2.58344 |

tions for the rates $\lambda_i$, $\beta_{i,j}$ and $\gamma_i$ are then derived from [5, Tables III-VI] in a straightforward manner, and we thus omit here their resulting expressions.

Our numerical results are summarized in Figure D.1 and Table D.2. In Figure D.1, we plot the probability mass function of the exact reproduction number $R_{exact,0}$ for the father, the mother and the children, in the cases of uncrowded, crowded and overcrowded families. Table D.2 lists the expected length $E[T']$ of an outbreak (in days), the mean number $E[N_{inf}]$ of infected individuals in steady state, and the expected value $E[R_{exact,0}]$ of secondary cases generated by various choices of the initial infective within uncrowded, crowded and overcrowded families.

It is then observed that, regardless of the tagged individual, the values of each probabilistic descriptor increase with the crowding of the housing conditions of a family. Regarding the various types of individuals within a family, the mother seems to play the less infective role during an outbreak, regardless of the housing conditions, and by contrast the children play the most infective role. However, there is not a clear monotonicity regarding the age of the child and its infectivity, although the youngest children seem to be more infectious than the oldest and middle children. The low infective role played by the mother (which is closely related to the probability mass function of $R_{exact,0}$ in Figure D.1 as well as to the mean duration of an outbreak and the mean exact reproduction number in Table D.2) seems to be accompanied by the more vulnerable role regarding the spread of the disease during an outbreak. Indeed, regardless of the type of the family and the individual who initiates an outbreak, the mother is the member of the family that suffers more infections after the beginning of an outbreak. This remark does not contradict the well-documented fact [5, Table V] that the youngest child is most often the primary case, since the exact reproduction number is a measure of transfer of infectivity within the family (that is, results in Figure D.1 and Table D.2 are related to an outbreak).

*Appendix D.2. On organizational aspects of intensive care units*

We study here a decision-making case regarding organizational aspects of ICUs. Based on concrete recommendations on basic requirements for intensive

care medicine (Valentin and Ferdinande [32]), we focus on a single ICU or a number of ICUs accommodating twelve intensive care beds, and the spread of a disease caused by nosocomial pathogens, such as *Staphylococcus aureus* (Chamchod and Ruan [6], Forrester and Pettitt [12], McBryde et al. [20]). Decisions concern especially the size of separate cubicles (common rooms) accommodating patients, and the number of nursing staff members and their responsibilities. In our examples, identical sizes are assumed for cubicles, which may accommodate a number $r$ of 1, 2, 3, 4, 6 and 12 intensive care beds. This leads us to divide the set of twelve beds into 12, 6, 4, 3, 2, and 1 cubicles, respectively. The number of intensive care nurses necessary to provide appropriate care and monitoring is calculated according to the following scenarios:

***Scenario A:*** Patients shall be able to be visualized at all times to facilitate detection of status changes and enhance implementation of therapeutic actions. This may be arranged from a single central nursing station, which results in a complete connected graph where the nodes correspond to the patients, and disease-causing internal infections are generated by either *indirect* contacts among patients due to the nursing staff and related responsibilities, or *direct* contacts among patients sharing the cubicle.

***Scenario B:*** The intensive care nurses are divided into a number of nursing stations, and each nursing station is only in charge of two *consecutive* cubicles. Cubicles can be then thought of as a circular connected graph since they communicate only with their neighbors.

For convenience, we assume that patients are homogeneous with respect to their recovery processes and disease-causing external infections, that is, $\gamma_i = \gamma$ and $\lambda_i = \lambda$ for nodes (patients) $1 \leq i \leq 12$, with $\gamma > 0$ and $\lambda > 0$. Patients accommodated in different cubicles, but under the case of a common nurse are assumed to have transmission-contact rates $\beta_{i,j} = \beta_{j,i} = a$, whereas $\beta_{i,j} = \beta_{j,i} = a + b$ in the case of patients belonging to the same cubicle; i.e., the term $a$ is associated with indirect contacts due to a common nurse, and infections caused by direct contacts for patients sharing a common cubicle are related to the term $b$.

Figure D.2 and Table D.3 are related to the parameters $\gamma = 1.0$ and $\lambda = 0.04$. More concretely, we display in Figure D.2 the probability mass function of $R_{exact,0}$ for values $a = 0.5$ and $b = 0.5$. Three selections for the cubicle size $r$ are considered for scenarios A and B. Similarly, Table D.3 lists the expected value of the exact reproduction number for cubicle sizes $r \in \{1, 2, 3, 4, 6, 12\}$ and scenarios A and B, with $a \in \{0.25, 0.5, 1.0\}$ and $b \in \{2^{-1}a, a, 2a\}$. For every fixed pair $(a, b)$, it is observed that the effect of the number $r$ of beds per cubicle on $E[R_{exact,0}]$ is not very significant in scenario A while, on the contrary, the value $r$ in scenario B is important for the spread of the disease in terms of secondary cases. The spread level of the disease – in terms of $E[R_{exact,0}]$ – behaves as an increasing function of the number $r$ of beds per cubicle, regardless of the selected values $a$ and $b$.

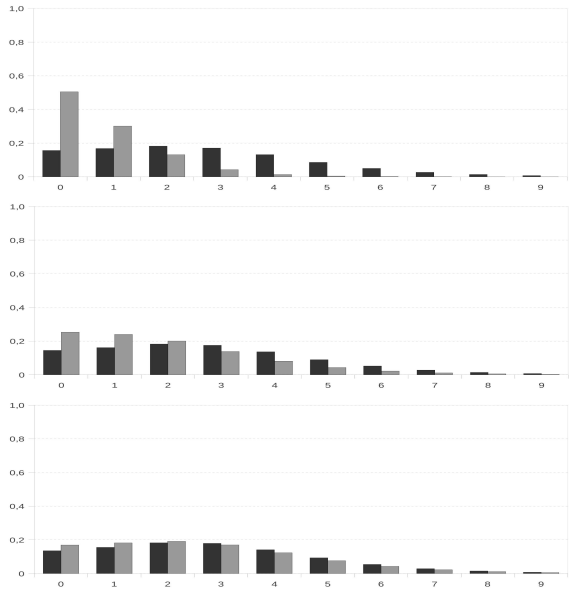


Figure D.2: Mass function of $R_{exact,0}$ for (*from top to bottom*) the cubicle sizes $r = 1$, 2 and 3, under the organizational assumptions in (*from left to right*) scenarios A and B.

As a general recommendation, we point out that scenario B shall be preferred to scenario A. Organizational aspects of the nursing staff seem to be more important than an appropriate selection of the number $r$ of beds per cubicle for a predetermined scenario; more concretely, it seems more beneficial to organize the nursing staff than reducing the cubicle size. However, differences in the values of $E[R_{exact,0}]$ between scenarios A and B become smaller with increasing values of the number $r$ of beds per cubicle. Note that identical values are derived for scenarios A and B in the cases $r \in \{4, 6, 12\}$ since the selection of $r$ in these cases turn the complete connected graph into a circular connected one.

## References

[1] Allen LJS (2003) An Introduction to Stochastic Processes with Applications to Biology. Pearson Education, Inc., New Jersey.

[2] Artalejo JR, Lopez-Herrero MJ (2013) On the exact measure of the disease spread in stochastic epidemic models. Bulletin of Mathematical Biology 75: 1031-1050.

[3] Artalejo JR (2014) On the Markovian approach for modeling the dynamics of nosocomial infections. Acta Biotheoretica 62: 15-34.

Table D.3: Mean exact reproduction number $E[R_{exact,0}]$ versus the cubicle size $r$, for scenarios A and B.

| $a$ | $b$ | Scenario | $r=1$ | $r=2$ | $r=3$ | $r=4$ | $r=6$ | $r=12$ |
|---|---|---|---|---|---|---|---|---|
| 1.0 | 2.0 | A | 3.29724 | 3.36793 | 3.42545 | 3.47469 | 3.55851 | 3.75751 |
| | | B | 1.29065 | 2.63125 | 3.19392 | 3.47469 | 3.55851 | 3.75751 |
| | 1.0 | A | 3.29724 | 3.34191 | 3.38185 | 3.41806 | 3.48210 | 3.63476 |
| | | B | 1.29065 | 2.56422 | 3.13718 | 3.41806 | 3.48210 | 3.63476 |
| | 0.5 | A | 3.29724 | 3.32251 | 3.34634 | 3.36890 | 3.41078 | 3.51730 |
| | | B | 1.29065 | 2.51577 | 3.08958 | 3.36890 | 3.41078 | 3.51730 |
| 0.5 | 1.0 | A | 2.74065 | 2.87201 | 2.97926 | 3.06935 | 3.21530 | 3.51730 |
| | | B | 0.78219 | 2.01537 | 2.69486 | 3.06935 | 3.21530 | 3.51730 |
| | 0.5 | A | 2.74065 | 2.81640 | 2.88440 | 2.94593 | 3.05357 | 3.29724 |
| | | B | 0.78219 | 1.89879 | 2.56781 | 2.94593 | 3.05357 | 3.29724 |
| | 0.25 | A | 2.74065 | 2.78155 | 2.82024 | 2.85690 | 2.92487 | 3.09552 |
| | | B | 0.78219 | 1.82451 | 2.47972 | 2.85690 | 2.92487 | 3.09552 |
| 0.25 | 0.5 | A | 1.97339 | 2.15071 | 2.30300 | 2.43500 | 2.65302 | 3.09552 |
| | | B | 0.43553 | 1.31602 | 1.98447 | 2.43500 | 2.65302 | 3.09552 |
| | 0.25 | A | 1.97339 | 2.07077 | 2.16074 | 2.24406 | 2.39342 | 2.74065 |
| | | B | 0.43553 | 1.19472 | 1.80817 | 2.24406 | 2.39342 | 2.74065 |
| | 0.125 | A | 1.97339 | 2.02458 | 2.07375 | 2.12101 | 2.21017 | 2.44132 |
| | | B | 0.43553 | 1.12439 | 1.69943 | 2.12101 | 2.21017 | 2.44132 |


[4] Austin DJ, Bonten MJM, Weinstein RA, Slaughter S, Anderson RM (1999) Vancomycin-resistant enterococci in intensive-care hospital settings: Transmission dynamics, persistence, and the impact of infection control programs. Proceedings of the National Academy of Sciences 96: 6908-6913.

[5] Brimblecombe FSW, Cruickshank R, Masters PL, Reid DD, Stewart GT (1958) Family studies of respiratory infections. British Medical Journal 18: 119-128.

[6] Chamchod F, Ruan S (2012) Modeling the spread of methicillin-resistant *Staphylococcus aureus* in nursing homes for elderly. PloS One 7, Article ID e29757, 8 pages.

[7] Ciarlet PG (1989) Introduction to Numerical Linear Algebra and Optimisation. Cambridge University Press, Cambridge.

[8] Cooper BS, Medley GF, Scott GM (1999) Preliminary analysis of the transmission dynamics of nosocomial infections: Stochastic and management effects. Journal of Hospital Infection 43: 131-147.

[9] Danon L, Ford AP, House T, Jewell CP, Keeling MJ, Roberts GO, Ross JV, Vernon MC (2011) Networks and the epidemiology of infectious disease. Interdisciplinary Perspectives on Infectious Diseases, Volume 2012, Article ID 284909, 28 pages.

[10] Darroch JN, Seneta E (1967) On quasi-stationary distributions in absorbing continuous-time finite Markov chains. Journal of Applied Probability 4: 192-196.

[11] Diekmann O, Heesterbeek H, Britton T (2013) Mathematical Tools for Understanding Infectious Disease Dynamics. Princeton University Press, Princeton, NJ.

[12] Forrester M, Pettitt AN (2005) Use of stochastic epidemic modeling to quantify transmission rates of colonization with methicillin-resistant *Staphylococcus aureus* in an intensive care unit. Infection Control and Hospital Epidemiology 26: 598-606.

[13] Gómez S, Gómez-Gardeñes J, Moreno Y, Arenas A (2011) Nonperturbative heterogeneous mean-field approach to epidemic spreading in complex networks. Physical Review E 84: Article ID 036105, 7 pages.

[14] Grimwood K, Abbott GD, Fergusson DM, Jennings LC, Allan JM (1983) Spread of rotavirus within families: A community based study. British Medical Journal 287: 575-577.

[15] Hill AL, Rand DG, Nowak MA, Christakis NA (2010) Emotions as infectious diseases in a large social network: the SISa model. Proceedings of the Royal Society B 277: 3827-3835.

[16] Hunter JJ (1983) Mathematical Techniques of Applied Probability. Discrete Time Models: Basic Theory, Vol. 1. Academic Press, New York.

[17] Keeling MJ, Eames KTD (2005) Networks and epidemic models. Journal of the Royal Society Interface 2: 295-307.

[18] Kephart JO, White SR (1991) Directed-graph epidemiological models of computer viruses. Proceedings of the 1991 IEEE Computer Society Symposium on Research in Security and Privacy, pp. 343-359.

[19] Latouche G, Ramaswami V (1999) Introduction to Matrix Analytic Methods in Stochastic Modeling. ASA-SIAM Series on Statistics and Applied Probability, Philadelphia.

[20] McBryde ES, Pettitt AN, McElwain DLS (2007) A stochastic mathematical model of methicillin resistant *Staphylococcus aureus* transmission in an intensive care unit: Predicting the impact of interventions. Journal of Theoretical Biology 245: 470-481.

[21] Meyers LA, Newman MEJ, Pourbohloul B (2006) Predicting epidemics on directed contact networks. Journal of Theoretical Biology 240: 400-418.

[22] Moslonka-Lefebvre M, Pautasso M, Jeger MJ (2009) Disease spread in small-size directed networks: Epidemic threshold, correlation between links to and from nodes, and clustering. Journal of Theoretical Biology 260: 402-411.

[23] Newman MEJ (2010) Networks. An Introduction. Oxford University Press, Oxford.

[24] Pautasso M, Moslonka-Lefebvre, Jeger MJ (2010) The number of links to and from the starting node as a predictor of epidemic size in small-size directed networks. Ecological Complexity 7: 424-432.

[25] Sahneh FD, Scoglio C, Van Mieghem P (2013) Generalized epidemic mean-field model for spreading processes over multilayer complex networks. IEEE/ACM Transactions on Networking 21: 1609-1620.

[26] Saito K, Kimura M, Motoda H (2009) Discovering influential nodes for SIS models in social networks. In: Discovery Science. Lecture Notes in Computer Science. Vol. 5808, pp. 302-316.

[27] Saito K, Kimura M, Ohara K, Motoda H (2012) Efficient discovery of influential nodes for SIS models in social networks. Knowledge and Information Systems 30: 613-635.

[28] Sharkey KJ, Fernandez CF, Morgam KL, Peeler E, Thrush M, Turnbull JF, Bowers RG (2006) Pair-level approximations to the spatio-temporal dynamics of epidemics on asymmetric contact networks. Journal of Mathematical Biology 53: 61-85.

[29] Simon PL, Taylor M, Kiss IZ (2011) Exact epidemic models on graphs using graph-automorphism driven lumping. Journal of Mathematical Biology 62: 479-508.

[30] Taylor M, Simon PL, Green DM, House T, Kiss IZ (2012) From Markovian to pairwise epidemic models and the performance of moment closure approximations. Journal of Mathematical Biology 64: 1021-1042.

[31] Taylor TJ, Kiss IZ (2014) Interdependency and hierarchy of exact and approximate epidemic models on networks. Journal of Mathematical Biology 69: 183-211.

[32] Valentin A, Ferdinande P (2011) Recommendations on basic requirements for intensive care units: structural and organizational aspects. Intensive Care Medicine 37(10): 1575-1587.

[33] Van Doorn EA, Pollett PK (2013) Quasi-stationary distributions for discrete-state models. European Journal of Operational Research 230: 1-14.

[34] Van Mieghem P, Omic J, Kooij R (2009) Virus spread in networks. IEEE/ACM Transactions on Networking 17: 1-14.

[35] Van Mieghem P, Cator E (2012) Epidemics in networks with nodal-infection and the epidemic threshold. Physical Review E 86: Article ID 016116, 10 pages.

[36] Vega-Redondo F (2007) Complex Social Networks. Cambridge University Press, New York.

[37] Verdasca J, Telo da Gama MM, Nunes A, Bernardino NR, Pacheco JM, Gomes MC (2005) Recurrent epidemics in small world networks. Journal of Theoretical Biology 233: 553-561.

[38] Watts DJ, Strogatz SH (1998) Collective dynamics of 'small-world' networks. Nature 393: 440-442.

[39] Wilkinson RR, Sharkey KJ (2013) An exact relationship between invasion probability and endemic prevalence for Markovian SIS dynamics on networks. PLoS ONE 8(7): e69028. DOI 10.1371/journal.pone.0069028

[40] Yates A, Antia R, Regoes RR (2006) How do pathogen evolution and host heterogeneity interact in disease emergence? Proceedings of the Royal Society B (Biological Sciences) 273, 3075-3083.

[41] Zhang X, Sun GQ, Zhu YX, Ma J, Jin Z (2013) Epidemic dynamics on semi-directed complex networks. Mathematical Biosciences 246: 242-251.